UNIVERSITY OF OKLAHOMA

GRADUATE COLLEGE

MANY-BODY DELOCALIZATION AND EVIDENTIAL STUDY IN POWER GRID

A DISSERTATION

SUBMITTED TO THE GRADUATE FACULTY

in partial fulfillment of the requirements for the

Degree of

DOCTOR OF PHILOSOPHY

By

GUOMIN JI
Norman, Oklahoma
2020

MANY-BODY DELOCALIZATION AND EVIDENTIAL STUDY IN POWER GRID

A DISSERTATION APPROVED FOR THE
SCHOOL OF ELECTRICAL AND COMPUTER ENGINEERING

BY THE COMMITTEE CONSISTING OF

Dr. John N. Jiang, Chair

Dr. Xingru Wu, Outside Member

Dr. Paul S. Moses, Member

Dr. Ronald Barnes, Member

Dr. Hjalti Sigmarsson, Member

Acknowledgment

During the research work over the past several years, I have received a big deal of support, assistance and encouragement from a great number of individuals. First of all, I would like to express my sincere gratitude to my advisor, Dr. John Jiang, whose consistent support and guidance have been invaluable throughout my study in OU since August 2017. Without his persistent support, the goal of this dissertation would not have been realized. His creative insights, and profound knowledge not only steered me through this research, but also set an excellent example, which motivates me to strive for excellence in future.

I would also like to extend my truthful thanks to all my committee members, Dr. Wu, Dr. Moses, Dr. Sigmarsson, and Dr. Barnes for their insightful comments, suggestions, and inspirations, which enabled me to improve my research from a variety of perspectives.

I also thank Dr. Yan Zhang and Dr. Sudantha Perera, who shared valuable thoughts and recommendations on my research during the collaborations on the projects. I am deeply indebted to Dr. Wu, who have been helpful of my research goals and who worked actively to provide me with the valuable academic time to pursue those goals.

Special thanks go to the faculties, staff, and classmates in the school of electrical and computer engineering and all my colleagues in my research group. I gratefully acknowledge close friends and classmates both in China and the USA. They always kept me accompanied and made my life being colorful.

Last but not least, I would love to express my deepest gratitude to my family. This work would not have been possible without their endless love and unconditional support. I am incredibly grateful to my husband. He is incredibly supportive and has made countless sacrifices to take good care of the family and help me focus on the research. I am so lucky to be graciously helped and supported by many people. I may leave out some

names that I should acknowledge, and I sincerely ask their forbearance and express my appreciation.

Guomin Ji

Table of Contents

List of Figures

List of Tables

Abstract

Complex energy flow dynamics following an untoward event has a direct impact on the responses of the protective and stabilization control systems of the power grid, in defending the power grid against from large-scale cascading failures or network fragmentation.

In this dissertation, a non-classic view and an analytical framework on electro-mechanical dynamics are proposed, which is different from the electric circuit-based ones built up classic physics.

Inspired from some recent advances in port-Hamiltonian formulism in control systems and random work interpretation of energy flows in electric circuit, a hypothetical but well-grounded unitary view on power grid is postulated, which leads to the new concept of many-body delocalization. The power grid with n ports of synchronized components can be transformed into a unitary electromagnetic field, which can be mathematically described by a complete graph that couples the active and passive resources and boundaries. Thus, the energy flow becomes the manifestation of an underlying unitary electromagnetic field.

A quantum number-based analytical framework is built based on several principles related to the unitary field view, such as Hermitian symmetry, Heisenberg uncertainty principles and general relativistic effect. With the intrinsic properties of the quantum number-based model, a new network property is developed, namely z-direction radical distance. This is a new concept about the projection of angular quantum number and the unit reference potential. This novel radical distance concept describes the fundamental connection between the energy flow in a complex network and its structure: it stands for the fraction of system energy surging at various spots as the result of l-motions along the z-direction, later found very useful for understanding the energy flow in power grid. An evidential experiment is carried out using a real world power grid model of electro-mechanical stability. With mathematical tools from tensor analysis of network,

the estimation of distribution of network energy flow in the power grid is derived. By comparing the radical distance based estimation of electromagnetic waves in the power grid to the one calculated with the complete dynamic system model of the power grid, a remarkable consistency is observed. This dissertation presents a unique perspective for complex network analysis, which is drastically different from the current "small-world" one. Based on its analytical root and the evidential experiments, we discover that radical distance is a metric that penetrates the boundary between the microscopic quantum world and real-world macroscopic power and energy systems. Such a discovery suggests the possibility of the coupling of active resources of power grid could be of the entangled particles type, authoring the usage of quantum effects in explaining and dealing with the states at a macroscopic scale, at least from a modeling/analytical perspective.

CHAPTER 1

Introduction

1.1 Research problem description

The energy flow is very important for power grid operations. Operators in large interconnected electric power systems aim to transfer scheduled power from one area to the other while adhering to the operating conditions that include security and economy. Power system operation in North America follows a framework set by the North American Electric Reliability Corporation (NERC) which requires security constraints to be fulfilled for different operating conditions. Generally the security constraints include static constraints such as thermal limits, and dynamic constraints such as voltage limits and transient stability limits [1]. Also, additional power can be transferred in case of contingency or other atypical operational conditions. These conditions suggest the significance of interface flows for planning as well as operational cases while satisfying security assessments [2].

In addition to the security constraints, one critical component of power system operation is the determination of maximum transfer capability, which remains significant for trading. Maximum transfer capability can be referred to the measure of ability of interconnected power system to reliably transfer power from one area to another [1]. This ability of interconnected transmission networks to reliably transfer electric power may be limited by the physical and electrical characteristics of the systems and can be majorly classified by thermal limits, voltage limits and stability limits. Once the critical contingencies are identified, the impact of these limits on the network is evaluated to determine the most restrictive. Here, thermal limits establish the maximum amount of electrical current that an interconnection can sustain over a specific time period. Ad-

ditionally, changes in voltage levels must be maintained within an acceptable range to avoid widespread system impact. Most of all, the ability of power system to survive disturbances is established by stability limits and is of major concern due to the changing dynamics of the system, specifically transient stability limits.

The power system is a highly non-linear system that operates in a constantly changing environment with variable loads, generator outputs and various operating parameters. Stability of such a system is dependent on the initial operating conditions when subjected to a disturbance, as well as on the severity of the disturbance. In large interconnected power systems, dynamic stability of energy exchange is of great significance for operation and planning purposes.

The determination of dynamic stability of energy exchange normally is based on the time domain simulated dynamic trajectories using electro-mechanical dynamic models. This is due to the fact that dynamic stability limit of energy exchange is concerned with the ability of the power system to maintain synchronism when subjected to a severe disturbance under the given initial operating state of the system [3]. Hence the determination and calculation of the dynamic stability of energy exchange is one of the most complicated and time consuming task. Moreover, since the conditions on the interconnected network changes continuously in real-time, the transfer capabilities need to be updated for every interface at regular intervals and hence requires the calculations to be fast and accurate [4].

The dynamic stability is one of the major factors that not only directly impact the system operating stability condition, they may also be a binding constraint that impact the outcomes of short-term markets and real-time generation dispatch solutions.

According to the classification of power system stability problems, the determination of limits for active power exchange is a electo-mechanical dynamical transient problem of frequency or angle stability which is described mathematically by a number of *Differential and algebraic equations* (DAEs). The electro-mechanical dynamic models are the

most sophisticated models for power system analysis.

The dynamic characteristics of energy flow in power grid are very complex due to the size of the system, the interconnection relationship of each components and the distinct dynamic characteristics of each components. For complex power grid, different components have distinct dynamic characteristics. Different dynamic problems have different models. As a result of the complexity, the dynamic characteristics of energy flow in power grid are needed to be fully understood.

1.2 Motivations and objectives

Understanding the dynamics of energy flow on interconnected electric power networks [5, 6] is a major and profound work with applications ranging from setting threshold of protective devices, determining various security limits for daily power grid operation, to making critical decisions on load shedding or grid sectionalization following an unexpected contingencies for prevention and mitigation of large-scale cascading failures.

Today, determination of the operating limits and control decisions rely on the experience of grid operators based on off-line time domain simulation studies. It has been a long-standing challenge to quickly identify the critical components in responses to the contingencies, particularly following a dramatic untoward change of system or real-time market operating condition. The limitation of time domain simulation becomes a more pressing concern for real-time needs nowadays as the grid operating condition becomes more fluctuating, due to the time and efforts needed for construction, modification, validation of models, in addition to the execution time of simulation and the massive amount of output data.

Moreover, the envisioned complexity of the next generation power grid will not easily be solved with computation and information technologies, not only because of the models of power grid may represent the interactions of hundreds of thousands of non-linear

components, also due to the fact that some of new components (such as fast-acting semiconductor-based power devices) cannot be adequately modelled with current analytics, particularly those associated with the transient behaviors of energy flow in the power grid.

To deeper understand the uncertainties and complexity of electric power grid dynamic stability, and better describe the relation between characteristics of energy flow and physics property of power grid in terms of modeling and method for solving practical problems, an novel electro-mechanical dynamic stability analytics is necessary.

1.3 Overview of contributions of dissertation research

The primary contributions of this research are summarized as follows:

- First of all, a common feature of the current State-of-the-Art is identified and some new explorations of the recent works are conducted.

- Next, a new integrated power grid hypothetical view is postulated. The view on synchronous electric power grid is a hypotheses permitting physics properties, with a goal of bring principles and models to bear on complex problems of energy flow on the power grid. The hypothetical view permits delocalizaiton of particles so that they can be considered as a single-particle level, like one with quantum particles that occupy different energy orbitals.

  Note that different from a small-world perspective on power grid, this unitary view is conceived as an undertaking towards a full first-principles account of a quantum or "quantumic" analytics for understanding some complex behavior of energy flow during transient period.

- Third, a quantum number-based (n-l-m) model for power grid based on this unitary electromagnetic field hypothesis is proposed.

- Furthermore, an estimation on a specific energy influx in the electric power grid using the quantum number-based (n-l-m) model is presented. Specifically, this study shows that under this hypothetical view, how the Heisenberg uncertainty principle [7] and quantum number-based (n-l-m) model can help us exploit the energy transient in electric power grid.

- At last, independent test studies in estimation of energy influx using real power grid models are presented and assert an industrial-grade accuracy of quantification.

1.4 Organization

This thesis is organized as follows. Chapter 2 presents the investigation results of the current major methods for dynamics stability analysis. Chapter 3 conducts some new explorations of recent works and an integrated power gird hypothetical view is postulated. Chapter 4 presents a quantum number-based (n-l-m) model. The chapter also presents the estimation of specific energy influx distribution. Chapter 5 is a practical application using experimental studies based on a real world power grid. Finally, chapter 6 draws a conclusion of the work and proposes the future work.

CHAPTER 2

Summary of Fundamentals for Current Analytics

2.1 Current major methodologies

In this section, two major analytics for power grid dynamic stability are reviewed. One is the electric circuit theory-based analytics. The other one is the complex network theory-based analytics.

2.1.1 Electric circuit theory-based analytics

Although more and more direct current (DC) energy systems are integrated such as DC transmissions and storages, the power grid currently is still considered as an alternating current (AC) interconnection under a given frequency of 50Hz or 60Hz. Such a power grid presents various types of energy transients or power flows, that are described mathematical with different electric circuit-based models according the theory of classic physics.

The current electric circuit theory-based analytics of power grid dynamic stability can be broadly categorized under two major types of approaches: 1) deterministic numerical simulation approaches [8, 9, 10, 11], and 2) direct methods [5, 12, 13].

2.1.1.1 Numerical simulation methods

The electro-mechanical dynamic models are the most sophisticated models for power system analysis, which consist a set of DAEs as shown in (2.1) and (2.2)

$$\dot{x} = F(x, y, \lambda), \tag{2.1}$$

$$0 = G(x, y, \lambda), \tag{2.2}$$

where x is vector of state variables that includes machine dynamic states, y is vector of network variables such as bus voltage magnitudes and angles, and λ is vector of parameters that are subject to change that includes load, generation or transmission line impedance.

Power systems are non-linear dynamic systems, whose behaviors are usually modeled by DAEs. The algebraic equations describe the network connectivity, network parameter, coordinate transformations used in generator equations, and all static elements, e.g. static loads. The differential equations describe the behaviors of all dynamic elements, including generators and their control systems, dynamic loads and FACTs (flexible alternating current transmission systems) devices.

For a power system with n_g synchronous generators, its dynamics can be described by a set of DAEs as shown in (2.3) and (2.4), while considering simplifying assumptions of constant rotor winding flux, constant mechanical torque and no damping.

$$\dot{\delta}_i = \omega_i - \omega_R, \text{ for } i = 1, \ldots, n_g \tag{2.3}$$

$$\dot{\omega}_i = \frac{1}{M_i}(P_{mi} - P_{ei}), \text{ for } i = 1, \ldots, n_g \tag{2.4}$$

where $\dot{\delta}_i$ and ω_i are the angle and angular velocity of the i^{th} machine, M_i is the inertial constant of the i^{th} machine, and P_{mi} and P_{ei} are the mechanical and electrical power of the i^{th} machine, respectively. ω_R is the reference angular frequency of the system. As known, the electrical power P_{ei} in (2.4) can be defined as,

$$P_{ei} = G_{ii}E_i^2 + \sum_{\substack{j=1 \\ j \neq i}}^{n} E_j E_i Y_{ij} \cos(\Theta_{ij} - \delta_i + \delta_j), \tag{2.5}$$

where E_i and E_j are the magnitudes of the voltages of electric machine at internal nodes i and j respectively; δ_i and δ_j are the angles of electric machines at node i and j respectively; Y_{ij} and Θ_{ij} is the magnitude and angle of the admittance between internal

node i and j respectively; lastly G_{ii} is the total conductance at internal node i.

Based on this conventional model, numerical simulation is the major approach to generate the rotor angle trajectories that will be used for determination of energy flow. In some advanced studies, different types of sensitivity are derived based on the analytical study to improve the computational efficiency.

Power system simulation methods have been used and the major methods in the electrical industry based on the power grid models including various components and considering economic factors to investigate the electro-mechanical dynamics.

Today, the operating energy flow stability is set mainly based on the results of off-line dynamic stability analysis obtained through time domain simulations.

The study of power systems in general might be difficult due to different time constants for different dynamic elements across the system. The time constants may range from 10^{-3} s for power electronic devices like FACTs to 10 s for governor system for controlling the active power input to generators. Here models representing static and dynamic characteristics of variety of power system components are discussed.

Synchronous generator model:

Two basic state variables of a generator are the rotor angle δ and the rotor speed ω. Since only the relative motions among different angles are of concern when analyzing the oscillation or angle stability, a rotating coordinate system at the synchronized speed/frequency is commonly used to represent the system equations, where the rotor speed $\Delta\omega$ is zero and rotor angle $\Delta\delta$ is a constant for each generator at the system equilibrium.

The generator model discussed here is a fourth-order differential equation with four state variables: δ, ω, e'_q and e'_d. The DAEs of a power system with m_g generators can be represented by the following set of equations,

$$\dot{\delta}_i = \omega_s \omega_i, \tag{2.6}$$

$$\dot{\omega}_i = \frac{1}{2H_i}(P_{mi} - P_{ei} - D_i\omega_i), \tag{2.7}$$

$$\dot{e}'_{qi} = \frac{1}{T'_{d0i}}\big(E_{fqi} - (X_{di} - X'_{di})i_{di} - e'_{qi}\big), \tag{2.8}$$

$$\dot{e}'_{di} = \frac{1}{T'_{q0i}}\big((X_{qi} - X'_{qi})i_{qi} - e'_{di}\big), \tag{2.9}$$

where δ_i, ω_i, e'_{qi} and e'_{di} are the rotor angle, rotor speed, transient voltages along q and d axes respectively of generator i; P_{ei}, i_{di} and i_{qi} are the electric power, stator currents of q and d axes respectively of generator i, which are functions of all rotor angles and network parameters; H_i and D_i are inertia and damping constants of generator i; T'_{d0i} and T_{q0i} are the open circuit time constants, X_{di} and X_{qi} are the synchronous reactance, X'_{di} and X'_{qi} are the transient reactance respectively for d and q axes of generator i; P_{mi} is the mechanical power of generator i; ω_s is the synchronized frequency of the system.

Since the above generator model is a fourth order model, it can accept exciter and governor to be incorporated in the model since it does not have field voltage as constant as opposed to a classical generator model that can only accept governor to the system. We briefly discuss the exciter and governor models in the following subsections.

Excitation system model:

The simplified IEEE type DC-1 excitation system [14] is shown in Fig. 2.1. The mathematical model is represented in the following equations,

$$\dot{E}_{fdi} = \frac{1}{T_{ei}}\big(V_{ri} - (K_{ei} + S_{ei}(E_{fdi})E_{fdi})\big), \tag{2.10}$$

$$\dot{V}_{ri} = \frac{1}{T_{ai}}\big(K_{ai}(V_{refi} - V_i - R_{fi}) - V_{ri}\big), \tag{2.11}$$

$$\dot{R}_{fi} = \frac{1}{T_{fi}T_{ei}}\Big(K_{fi}V_{ri} - K_{fi}E_{fdi}(K_{ei} + S_{ei}E_{fdi}) - R_{fi}T_{ei}\Big), \tag{2.12}$$

where V_{ref} is the reference voltage of the automatic voltage regulator (AVR); V_r and R_f are the outputs of the AVR and exciter soft feedback; E_{fd} is the voltage applied to generator field winding; T_a, T_e and T_f are AVR, exciter and feedback time constants;

K_a, K_e and K_f are gains of AVR, exciter and feedback; Vr, min and Vr, max are the lower and upper limits of V_r.

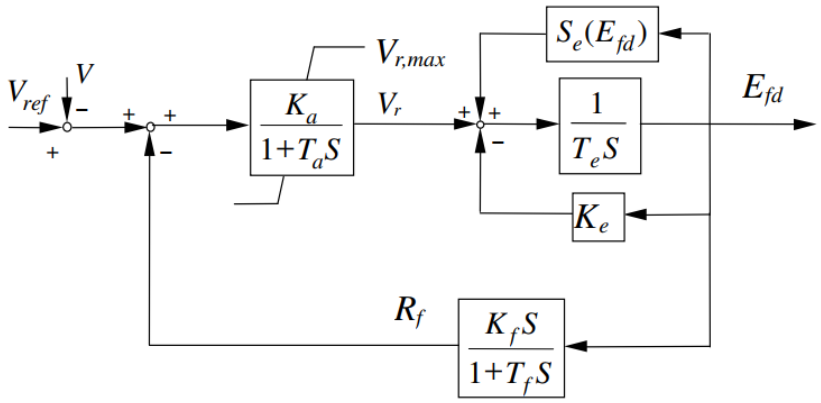

Fig. 2.1: IEEE type DC-1 Excitation System.

Governor system model:

A simplified prime mover and speed governor is shown in Fig. 2.2. The dynamics of a governor can be described by the following two differential equations,

$$\dot{P}_{mi} = \frac{1}{T_{chi}}(\mu_i - P_{mi}), \tag{2.13}$$

$$\dot{\mu}_i = \frac{1}{T_{gi}} - \frac{(\omega_i - \omega_{ref})}{R_i} - \mu_i. \tag{2.14}$$

In the formulations, the variable P_{mi} is the mechanical power of the prime mover and μ_i is the steam valve or water gate opening; R_i is the governor regulation constant representing the inherent speed-droop characteristic; ω_{ref} is the governor reference speed; T_{chi} and T_{gi} are the time constants related to the prime mover and speed governor respectively.

Remarks on time domain method:

A set of DAEs are numerically solved to study the transient behavior of power systems. As we know, power systems networks typically include thousands of generators, exciters, governors, loads, transformers and other devices, where each individual com-

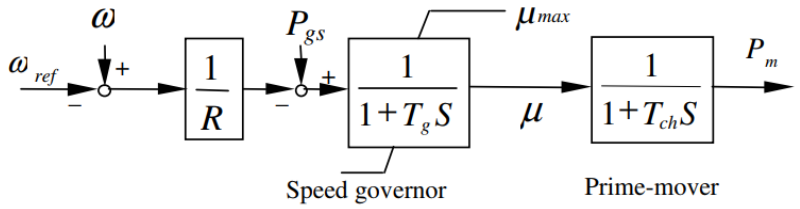

Fig. 2.2: Simplified speed governor and prime-mover.

ponent may need several differential and algebraic equations to represent, thus the total number of differential and algebraic equations of a real power system can be formidably large. These simulations also include step-by-step numerical integration of DAEs due to which errors may accumulate thereby yielding qualitatively wrong results. In this context we introduce different perspectives in order to avoid complex models for different components and move towards a uniform representation of key components in power system.

The simulation-based methods may not meet all the operational requirements in real-time, especially when the system operators need to make a rapid control or mitigation decisions in complicated operating conditions, such as untoward events.

The examples of time domain approaches are maximum rotor angle deviation and critical clearing time (CCT) that need full-scale time-based simulations which proves to be computationally taxing as well as time consuming. Additionally, time domain approaches fail to provide stability margins directly, determination of which requires full time domain simulations for the development of equivalent single-machine infinite-bus system for multi-machine system.

2.1.1.2 Direct energy function methods

The direct energy function methods [5, 12, 13] have recognized to be reliable and regarded a promising tool for dynamic stability analysis in power grid. The basis of the method is the famous Lyapunov's direct method [15] by constructing a scalar Lyapunov

or energy function $V(x)$,

$$\begin{aligned} V(\theta,\tilde{\omega}) =& \frac{1}{2}\sum_{i=1}^{m} M_i\tilde{\omega}_i^2 - \sum_{i=1}^{m}\int_{\theta_i^s}^{\theta_i} f_i(\theta)d\theta_i \\ =& \frac{1}{2}\sum_{i=1}^{m} M_i\tilde{\omega}_i^2 - \sum_{i=1}^{m} P_i(\theta_i-\theta_i^s) - \sum_{i=1}^{m-1}\sum_{j=i+1}^{m}\big[C_{ij}(\cos\theta_{ij}-\cos\theta_{ij}^s) \\ & - \int_{\theta_i^s+\theta_j^s}^{\theta_i+\theta_j} D_{ij}\cos\theta_{ij}d(\theta_i+\theta_j), \end{aligned} \tag{2.15}$$

which generally the sum of the kinetic and potential energies ($V_{KE}(\tilde{\omega}) + V_{PE}(\theta)$) of the post-fault system described by a set of three differential equations as below,

$$\dot{x}(t) = f^F(x(t)) \quad 0 < t \leq t_{cl} \tag{2.16}$$

with the initial condition $x(0) = x_0$, and

$$\dot{x}(t) = f(x(t)) \quad t > t_{cl} \tag{2.17}$$

with the initial condition $x(t_{cl})$ for Eq. (2.17) provided by the solution of the faulted system described in Eq. (2.16) evaluated at $t = t_{cl}$. The basic idea is to describe the interior of the region of attraction of the post-fault system (Eq. (2.17)) through an inequality of the type $V(x) < V_{cr}$. There are three basic methods to calculate the critical energy V_{cr}, which are 1) Lowest energy u.e.p method [16], 2) Potential Energy Boundary Surface (PEBS) method [17] and, 3) Controlling u.e.p method [18].

On the other hand, direct approach does not completely rely on time domain simulations and has the capability to restrict the time domain simulation for the period of disturbance, therefore considerably reducing the computational effort and time consumption. While other deterministic studies follow repeated time-based solutions that may result in computationally heavy and not so accurate results.

2.1.1.3 Remarks

Numerous research works have shown that the trajectory sensitivity approach can effectively complement time domain simulation and provide valuable insights in evaluating limits and account for changes in operating conditions and system parameters. However, there are several intrinsic challenges that are associated with the fundamental way of thinking which is based on the DAEs-based conventional framework of the power system dynamics analyses as listed below,

- Even with the support of advanced sensitive approaches, determination of the security boundary requires repeated time domain simulations taking into consideration of many operating conditions, which is time consuming.
- Conventional methods are highly dependent on the accuracy of presumed models for individual components. As a result, the methods suffer from the inaccuracy caused by modeling assumptions and the difficulties of state and parameter estimations.
- The entanglement of the different types of variables and states makes it difficult to develop an appropriate systematic approach to investigate the problems.
- Fundamentally, the electric circuit based models used in the conventional methods are derivatives from the presumed physics models which could cause errors in representing the nature of underlying physics or actual behavior of electric-magnetic energies dynamics in complex networks.

2.1.2 Complex network theory-based analytics

Complex network theory-based analytics is different electric circuit theory-based analytics from the fundamental perspective.

Applying complex network theory in development of new kind of analytics have attracted substantial attentions for the electric power engineering industry (as fast technology) and in network sciences (as understanding). Early research works have shown that complex network methods can be used to convert raw or processed information to support some long-term planning work of power grid and visualizing its layout with a satisfied accuracy [19, 20, 21]. Owing to many successful applications in analyzing a number of real complex systems, such as world-wide web, the internet, biological, and social networks, it has been holding high promise for long-standing or new challenges with high complexity such as prevention and mitigation of cascading failures, which demand a new analytical ways that do not relay on non-time-domain simulations, so the stability can be rapidly identified adaptively based on real-time operating condition without the much modeling efforts.

Organizations has created significant interest in whether there exist universal properties of networks that may be discovered and then applied to understand and manage them, that cannot be easily achieved based on current technology. It is also hoped that application of complex network theory can offer in-depth insights and inspirations for development of new science and technology breakthroughs.

The ubiquity of complex network theory across many science and practical engineering areas has attracted strong interests and motivated substantial efforts to exploit if there exist universal structural properties of networks, known or to be discovered, that can be used to better model, predict and address some dynamic transient energy flow related problems [19, 20, 21] of the power grid and dynamics of network itself. For example, a substantial amount of work including our prior ones have been focusing on applying complex network theory and properties to study cascading failures, vulnerability assessment [22, 23] and resiliency, that are related to complex dynamics of energy transient on the power grid.

One of the areas that have been studied intensive for over a decade is to understand

the dynamics of energy flow and its impact on cascading failures by applying some fundamental property of interdependent networks in illustration the possible cascading failures of dependent nodes [22, 23] including our prior work [24] .

2.1.2.1 Approach to power grid analysis with network indices

The foundation of complex network theory-based analytics is based on graph connection. A number of recent studies have used the concepts of network science and graph theory to understand the operational behavior of power system networks and further there have been efforts to establish links between the topological structure of power networks and vulnerabilities in the network [25, 26].

Electric power system structure can be represented by a graph G=($\mathscr{V}$,$\mathscr{E}$), constructed by assigning ports to each of the components, and the edges to the connections of electric power system structure, which is shown in Fig. 2.3 [27].

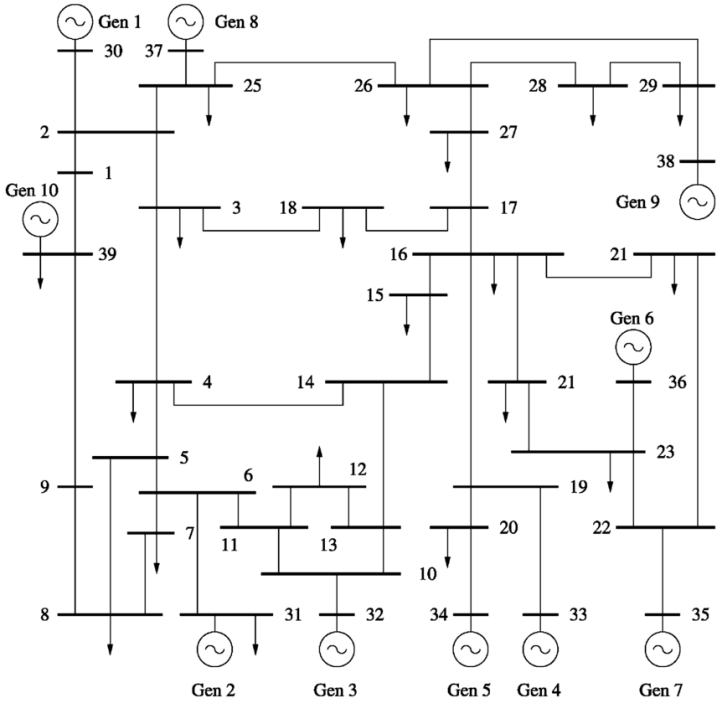

Fig. 2.3: Electric power system example.

In the general network representation of the electric power system, $\mathscr{V} = \{v_1, v_2 ... v_n\}$ and

$\mathscr{E} = \{e_1, e_2 ... e_m\}$ are denoted as the set of nodes and edges of network G respectively. $e_k(v_i, v_j)$ is denoted as the function of edge e_k leaves source vertex v_i and enters terminal vertex v_j. $n = |\mathscr{V}|$ and $m = |\mathscr{E}|$ denoted as the number of nodes and edges of network G respectively.

An graph, G=($\mathscr{V}$,$\mathscr{E}$), can be normally described by incidence matrix $\mathbf{M} = (M_{kh})$, $\mathbf{M} \in$ $\in \mathbb{R}^{M \times N}$ that denotes the incidence of edges on nodes, adjacency matrix $\mathbf{A} = (A_{ij})$, $\mathbf{M} \in \mathbb{R}^{n \times n}$ which denotes whether pairs of nodes are adjacent or not, and Laplacian matrix $\mathbf{L} = (L_{ij})$, $\mathbf{L} \in \mathbb{R}^{N \times N}$ that denotes the connection of nodes and edges. They can be defined as,

$$M_{kh} = \begin{cases} +1 & \text{if } v_h \text{ is the terminal node of edge } e_k \text{ ,} \\ -1 & \text{if } v_h \text{ is the source node of edge } e_k \text{ ,} \\ 0 & \text{otherwise.} \end{cases} \tag{2.18}$$

$$A_{ij} = \begin{cases} 1 & \text{if } v_i v_j \in \mathscr{E}, \\ 0 & \text{otherwise.} \end{cases} \tag{2.19}$$

Laplacian and adjacency matrix of a network are related by

$$\mathbf{L} = \mathbf{D} - \mathbf{A} = \mathbf{M}^T \mathbf{M}, \tag{2.20}$$

$$L_{ij} = \begin{cases} -1 & \text{if } v_i v_j \in \mathscr{E}, \\ D_{ii} & \text{if } i = j, \\ 0 & \text{otherwise,} \end{cases} \tag{2.21}$$

where $\mathbf{D} = (D_{ij})$ is the degree matrix, $\mathbf{D} \in \mathbb{R}^{n \times n}$, which is a diagonal matrix of the degrees of the nodes in the network.

The connection of node and transmission line in the electric power system can be denoted by the un-normalized Laplacian matrix in the network representation, which does not contain any weight shown in Eq. (2.20) and Eq. (2.21).

Knowing from above relationships of different matrices, the square of the Laplacian can be expressed as,

$$\mathbf{L}^2 = \mathbf{D}^2 - \mathbf{AD} - \mathbf{DA} + \mathbf{A}^2. \tag{2.22}$$

Next, we would like to show that the sign structure of $\mathbf{L}^2$ can be used to find the topology. Let's define the sign structure of a matrix $\mathbf{T} = (t_{kh})$, $\mathbf{T} \in \mathbb{R}^{n \times n}$ with notation $\text{sign}(\cdot)$, i.e., $\text{sign}(\mathbf{T}) = (\text{sign}_{kh}(\mathbf{T}))$, such that

$$\text{sign}_{kh}(\mathbf{T}) = \begin{cases} 1, & \text{if } t_{kh} \text{ is negative.} \\ 0, & \text{otherwise.} \end{cases} \tag{2.23}$$

Using the definition of the sign structure of a matrix, we known that

$$\text{sign}(\mathbf{L}^2) = \text{sign}(-\mathbf{AD} - \mathbf{DA}). \tag{2.24}$$

Since the degree matrix of the graph for electric power distribution system shown in Fig. (2.3) is positive-definite, then we know the following relationship,

$$\text{sign}(\mathbf{L}^2) = \mathbf{A}. \tag{2.25}$$

Eq. (2.25) shows that the adjacency matrix A can be constructed from L^2 matrix. Once the adjacency matrix is known, the topology is identified. Therefore, we could use sign structure of $\mathcal{L}^2$ matrix to represent the connection of power distribution networks.

Classification of network structures have recently been studied in fields of complex

networks science, social networks, etc. Also a number of recent studies have used the concepts of network science and graph theory to understand the operational behavior of power system networks and further there have been efforts to establish links between the topological structure of power networks and vulnerabilities in the network [25, 26]. For example, [25] provides a general concept of topology identification that takes into account shortest distance between two nodes, [28] introduces a centrality measure that defines the system based on its electrical topology, [29] and proposes a set of electrical betweenness measures which takes into account flow direction in power grids. While these studies provide substantial information regarding the structure of power system, the new research has shown that these models based on the foundation of complex network science lack in showing the operational aspects of the dynamics in power system.

2.1.2.2 Application in stability analysis with structural information

Structural analysis is an analytics of power system analysis that is based on structure of the electric power grid and does not depend on electric-circuit models and time domain simulations.

A new perspective of power gird dynamic stability analysis

The functional forms of different power system models defined under different operating conditions are based on basic electrical circuit laws i.e. KVL and KCL. Specifically, the active power flow equation shown in (2.26) is the most commonly used equation and is derived from Kirchhoff's current law.

$$P_i = V_i \sum_{j=1}^{n} V_j (G_{ij} \cos(\Theta_i - \Theta_j) + B_{ij} \sin(\Theta_i - \Theta_j)), \tag{2.26}$$

$$Q_i = V_i \sum_{j=1}^{n} V_j (G_{ij} \sin(\Theta_i - \Theta_j) - B_{ij} \cos(\Theta_i - \Theta_j)). \tag{2.27}$$

Such steady state equation can be solved mathematically but in many real-time ap-

plications this is simplified under a number of assumptions that result in DC power flow equations. These assumptions are 1) for normal operating conditions, assuming adequate reactive power that maintains the voltage magnitudes close to unity, and 2) neglecting resistances as compared to the reactances since transmission lines have high reactance. These assumptions remain valid for the small time window which allows us to use them for transient analysis when seen in a very small time interval since it behaves in a manner similar to steady-state perspective.

Nevertheless, for short-time period under relatively normal operating condition, the DC power flow equation has this form which can be seen as the simple uniform representation of the power system and its power flow. From a DC power flow perspective, apart from considering one per unit voltage magnitude at each bus and $G_{ij} = 0$, the difference of phase angles $(\Theta_i - \Theta_j)$ between two buses i and j is very small such that $\sin(\Theta_i - \Theta_j) \approx$ $\approx (\Theta_i - \Theta_j)$. This reduces the power flow problem in (2.26) to a linear equation as shown in (2.28),

$$P_i = \sum_{j=1}^{n} B_{ij}(\Theta_i - \Theta_j), \text{ or } \mathbf{P} = \mathbf{B}\boldsymbol{\Theta}, \tag{2.28}$$

where B_{ij} is the element in susceptance matrix $\mathbf{B}$. Therefore, from the classic view, Electric power system can be described by the admittance matrix, which is developed by applying KCL at each bus in the system and gives the relationships between all the bus current injections and all the bus voltage [30],

$$\mathbf{B}_{n\times n} = \begin{cases} B_{ii} = b_i + \sum\limits_{j=1, j\neq i}^{n} b_{ij}, & \text{if } \ i = j \\ B_{ij} = -b_{ij}, & \text{if } \ i \neq j \end{cases} \tag{2.29}$$

where b_i and b_{ij} are the susceptance of node i and transmission line connecting node i and node j.

Here matrix $\mathbf{B}$ defines the structure of the network and from the previous studies and the

functional forms of models representing different operating conditions, we can see that structure plays an important part in characterizing the performance of power system.

The traditional time domain methods and and deterministic methods have major computational issues and on-line real-time applications, which may face challenges due to these fundamental computational limitations. Therefore, digressing from conventional use of classic power flow based dynamic stability simulation approaches, a new method that is so called structural analysis is used to quantify the relationships between the active power transfer limits and dynamic transient stability. Specifically, the direct approach utilized in the analysis is transient energy based criteria which focuses on the quantitative measurement of the stability degree. A structural analysis based methodology is developed for 1) estimation of the transient stability interface limits based on structural stability of the grid from a system-wide perspective, and 2) identification of the weak spots or links in the grid structure for estimation of stability margins of generator and decision of controlled compensation at given operating conditions such as levels of the load, power generation and active power flow over the interface.

Overview of structural analysis

Structural analysis is an analytical approach of power system analysis that studies the dynamics of energy flow in a network from a topological perspective. Rather than relying on electric-circuit model and simulation methods, structural analysis relies on the topology of physical connection of power grid and related physics principles. Technically, structural analysis includes 1) embedding of information of power grid and operating condition (from measurement or simulation perspective) into undirected graph and matrix, 2) coordinate transformation which converts the matrix of the original graph to one that represents a completely graph, 3) application of fundamental physics principles to analyze the energy flow in the power grid. By taking the advantage of graph matrix formulism, quantitatively structural analysis only involves standard matrix operations and simple arithmetic so the computational burden is kept to a minimum. These mathemat-

ics tools allow us to develop ideas, equations and computational methods for analyses of issues related to energy flow over power network from a structural perspective.

In the research of our group, structural analysis was used to create a mathematical formula based on the matrices of original and converted graphs, for calculation of amount of energy exchanges among ports of generator during the initial period of the electromagnetic transient following a disturbance, or a fault-induced change of system potential (E_f), to compute fractal pattern of energy distribution, without using time domain simulations. Although for comparison purpose steady-state power system models and power flow simulation were still used to obtained the information about topology of power grid and system status, these information can be easily obtained through measurement for creation of the fractal pattern. In addition, structural analysis was used for estimation of the linking strengths of individual components of interest based on their topological locations and the composite of neighbors (from an electric-magnetic distance or topology perspective). Component linking strength ($W_{PE,i}^{max}$) is defined as the capability of individual component, in terms of potential energy, to support the additional inrush exchange of induced fault energy E_f at the corresponding ports. Finally, the information of induced fault energy distribution and component linking strengths, are used in the stability analysis.

Structural analysis is a physics-based analytics for power system analysis. Different from the conventional electric circuit based methods, in structural analysis, rather than simulating the variations of frequency, power and voltage angles over time using mathematical models described with DAEs, we directly create fractal patterns of energy distribution over network, compute the maximum energy exchanges at the ports of individual components as well as the linking strengths, and analyze the dynamic stability based on fundamental physics laws.

An conceptual application of structural analysis: transient energy automaton

Automata theory was established in the 20th century when mathematicians began de-

veloping machines which imitated a human perception of completing calculations more quickly and reliably [31]. Through automata, it is easy to understand how machines compute functions and solve problems and more importantly, what it means for a function to be defined as computable.

Automatons are abstract models of machines that perform computations on an input by moving through a series of states or configurations [31, 32]. At each state of the computation, a transition function determines the next configuration on the basis of a finite portion of the present configuration. As a result, once the computation reaches an accepting configuration, it accepts that input. The most general and powerful automata is the Turing machine. The main objective of automata theory is to develop methods by which we can describe and analyze the dynamic behavior of discrete systems, in which signals are sampled periodically. The behavior of these discrete systems is determined by the way that the system is constructed from storage and combination of elements. The automata theory has also been utilized in mathematical idealizations of nature systems, known as cellualar automata, which are designed to follow predetermined set of rules [33, 34, 35].

One of the main forms of automata is finite-state automata [36] which lays the foundation of transient energy automata.

Construction of transient energy automaton

The concept of transient energy automaton (TEA) [37] involves representation of a system as a graph with each vertex in the graph of TEA considered to be capable of processing energy by either reflection or absorption. When a vertex in the graph receives energy from the graph, this vertex has a tendency to absorb or reflect the received energy. That is, one vertex will absorb parts of the received energy while reflect another parts of the received energy to the other vertices on the graph. Therefore, the two actions can be termed as, *fast action* and *slow action*, to present the process of energy reflection and energy absorption.

The fast and slow actions of one vertex in the TEA network can be defined as:

- *Fast Action:* A process that after a vertex receives energy, a part of the received energy is reflected from a vertex and injected to the other vertices in the graph.
- *Slow Action:* A process that after a vertex receives energy, a part of the received energy is absorbed by this vertex.

The two actions on a vertex are coupled with each other and require complex rules governing them. In order to simplify and implement those actions into TEA model, the following rules are defined for coupling of two actions:

- The fraction of energy that can be absorbed by each vertex in the slow action or absorption ratio depends on the capability of the vertex;
- For each vertex, the amount of energy received at a local site (from the disturbance vertex or the reflected energy to neighboring vertices) or dispersion ratio in the fast action is a function of the graph geometry including the structure of lattice and value configuration of edges;
- Such rules are functions of the geometry and value configuration of graph and the property of vertices, and ultimately enable the TEA to create time evolution of energy distributions that may affect the dynamics of the system.

In summary, the first rule shows the absorption ratio is given by the property of that vertex, which is assumed to be known; the second rule shows dispersion ratio is related to graph geometry; the third rule shows the time evolution of TEA.

2.1.2.3 Remarks

In structural analysis, various graph representations have the advantage of allowing use of linear algebra and matrix operation for fast coordinates transformations and

computation of interactive energy exchanges, which makes the computation burden far more less and it also provides more reliable and robust numerical results. Moreover, the graph representation allows us to connect our knowledge of power system engineering to some fundamental physics, develop a insights on energy flow over network such as the random walk interpretation we proposed in our previous work, in additional to the understanding obtained from electric-circuit theory.

Although it can be demonstrated that complex network based methods can be used to provide some insights on the failures mechanisms, for example a broader degree distribution increases the vulnerability of interdependent networks to random failure, which is opposite to how a single network behaves. For example, our prior work on integrating more important variables in power system analysis to the complex network method yields an improved estimation results based on the standard methods of complex network. However from a more practical perspectives, we found it is very difficult to get exact analytical solutions for the critical fraction of nodes that, on removal, will lead to a failure cascade and to a complete fragmentation of two interdependent networks that can be used for real world of power system operation.

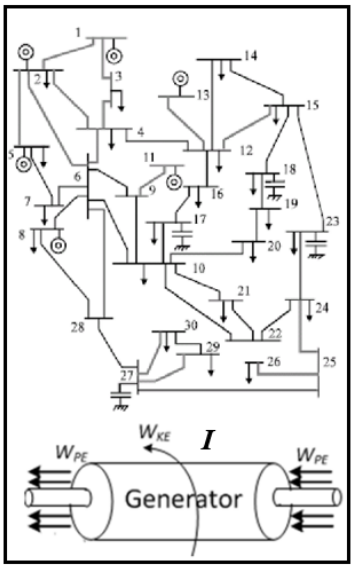

Fig. 2.4: Classic power gird and generator model.

There are on-going undertakings of seeking solutions from complex networks theory and

properties of complex networks to address some transient energy influx related complex network problems, such as cascading failures and vulnerability assessment of power grid [22, 23, 24].

The outcomes of current applications of complex networks theory in real world problems have created both excitement and confusion about to what extend the knowledge of network structure can be applied to describe and predict the energy transients to address practical issues. For example of a recent work of seeking network-based solutions to practical problems as found in [24] as well as many others, that complex network based methods can still be refined for a better description of dynamics and improved in prediction of critical components of power grid with appropriate integration of more engineering knowledge or variables such as direction and magnitude of power flow.

For example in [24], an exploration of if additional engineering factors can be incorporated in universal proprieties of complex networks and used to address some practical solutions to vulnerability of realistic power grid, we develop a method that the magnitude and direction of power flow into the major network models was presented and applied the analytical approach to an experiment of identification of critical nodes and their dependence sequence that, on failure, would cause cascading effects and network fragmentation. The experimental results are both exciting and confusing: it was exciting that the results showed that the proposed method is more effective comparing to the existing ones in terms of identification of nodal criticality and network vulnerability, which is not very surprising as more information about the dynamics on the network was appropriately used.

On the other hand, we also found the results were also confusing as that, although our approach yields better results and easy to implement than the major existing network-based approaches. However, most of these complex networks methods offer few additional insights to the real world problems other than what have been already known with the existing engineering methods, significant technical advantages in solv-

ing real problems, nor major superior prediction advantages comparing to the existing engineering methods for practical use.

Moreover, within the standard complex network setting of small-world, it was noticed that some critical factors impacting transient energy flow have not been adequately considered and normally has been ignored/excluded in most literature. Such as heterogeneity of network (a critical variable for system stability) caused by an uneven distribution of synchronous machine moment of inertia, is difficult to integrate into in existing network models and properties shown in Fig. 2.4. Fig. 2.4 is an example of single line diagram of IEEE system for a K-buses power grid with N ports, $K = 30, N = 6$. The bottom of Fig. 2.4 is a generator model. Further studies shows that neglecting these factors in network-based approaches seriously limit the applicability of classic complex network theory in address practical transient problems in real power grid.

Despite some pioneering conceptual works that demonstrated the potentials of complex network theory, there continue lack general answers to practical large weighted and directed networks, which most commonly emerge in complex systems. Although it can be demonstrated that complex network based methods can be used to provide some insights on the failures mechanisms, for example a broader degree distribution increases the vulnerability of interdependent networks to random failure, which is opposite to how a single network behaves. People continue seeking general network based solutions real world complex systems like the power grid.

2.2 An interpretation of common features

The common feature of the current major analytics of dynamic stability is the network structure. Network structure feature can be explained with port-Hamiltonian.

Motivated by the excitements and confusions, people continue exploiting if there exist universal structural properties of complex networks, known or to be discovered, that

can be applied to real complex network. The following two important observations on some recent works are made.

One of the recent investigations on the network representation of major power system models highlights the connection between traditional electric circuit theory-based approach and complex network theory-based application in power system analysis. It can be shown mathematically almost all existing models of power system analysis can be reformatted into uniform port-Hamiltonian representation [38], characterized by the interconnection matrices (i.e., the Laplacians), which are the impedance of transmission lines or branches.

It is known that electric power system can be viewed as a complex system network. In the complex network, port-Hamiltonian representation is very useful as an effect and unified method to analyze the complex network characteristics. Many of the models of the complex system can be converted into a port-Hamiltonian formulism. According to the general port-Hamiltonian formulism, it is clear that the system structure plays an import role to determine the performance of the network system [38, 39, 40, 41]. As I mentioned that power system is also a complex system, many of the problems are also can be represented by the port-Hamilton method. Therefore, the system structure is also an significant factor in the analysis of the electric power system dynamic characteristics, which is suggested by the literatures [42, 43].

A port-Hamiltonian formulations as one of the best representation of the dynamic system have been paid much attention [38, 39, 40, 41]. The port-Hamiltonian theory provides a systematic framework for the geometric description of network models of complex physical system. The idea of structural analysis can be explained using Port-Hamiltonian formulism. The framework of port-Hamiltonian systems combines the original framework by associating it with the network structure.

The port-Hamiltonian systems are open dynamical systems which can interact with their environment through ports and are a representation of the energy in a particular

network [44]. Therefore, an electrical network can be formulated as a port-Hamiltonian system. In order to formulate such systems, classical Hamiltonian equations are represented in the form of port-Hamiltonian system. Hamiltonian formulism is known as a general energy-based modeling approach in control systems. The standard Hamiltonian equations for a system in general form are given as,

$$\begin{cases} \dot{q} = \frac{\partial H}{\partial p}(q,p), \\ \dot{p} = -\frac{\partial H}{\partial q}(q,p) + B(q)f, \ \ f \in \mathbb{R}^m, \end{cases} \tag{2.30}$$

where the Hamiltonian $H(q,p)$ is the total energy of the system, $q = (q_1, \cdots, q_k)^T$ are generalized configuration coordinates for the dynamic system with k degrees of freedom, $p = (p_1, \cdots, p_k)^T$ is the vector of generalized momentum, and $B(q)f$ denotes the generalized forces resulting from the input $f \in \mathbb{R}^m$.

Port-Hamiltonian formulism is a modeling technique that adopt a port-energy based approach to convert the original models of interconnected components into Hamiltonian equations, which offers the following useful advantages for illustration of the idea of structural analysis,

1) Uniformity and additivity:

   Taking the advantage of energy additivity, port-Hamiltonian formulism offers a uniform way to construct a mathematical representations for a network of multi-physics energy system and its sub-systems with different dimensions and characteristics

2) Embedding of structural information:

   As a simplistic topological formulism, port-Hamiltonian offers geometric view of many dynamic systems and embedding of structural information of energy networks, which can be used to characterize their complex dynamics.

2.2.1 Uniformity in port-Hamiltonian formulism and features

As one of the energy-based modeling techniques, Port-Hamiltonian can convert the most models of dynamic systems into a following port-based representation [44]. Recent studies present the formulation of the electric power system as a unified port-Hamiltonian system that describes the dynamics of the electric network [42, 43, 45]. For example, the dynamics of the electrical network can be represented in Hamiltonian form as below [42],

$$\begin{bmatrix} \dot{q(t)} \\ \dot{\varphi(t)} \end{bmatrix} = \begin{bmatrix} 0 & \mathbf{J}_{LC} \\ \mathbf{J}_{LC} & 0 \end{bmatrix} \begin{bmatrix} q(t) \\ \varphi(t) \end{bmatrix}, \tag{2.31}$$

where $\mathbf{J}_{LC}$ represents $\mathbf{J}\mathbf{L}^{-1}$ or $\mathbf{J}^T\mathbf{C}^{-1}$ and C_i is the capacitance of the i^{th} capacitor, L_j is the inductance of the j^{th} inductor and $\mathbf{C} = \text{diag}(C_1 \cdots C_{n_C})$ and $\mathbf{L} = \text{diag}(L_1 \cdots L_{n_L})$. $q(t) \in \mathbb{R}^{n_C}$ and $\varphi(t) \in \mathbb{R}^{n_L}$ are vectors of capacitor charges and inductor fluxes at time t respectively. $\mathbf{J}$ is the skew symmetric $n \times n$ matrix defined by

$$\mathbf{J} = \begin{bmatrix} 0 & \mathbf{M} \\ -\mathbf{M}^T & 0 \end{bmatrix}, \tag{2.32}$$

where $\mathbf{M}$ is the incidence matrix of represented network of electric power system, which is shown in Fig. 2.5. The result interconnection matrix (Laplacian) can be seen as a weighted graph that explicitly represents the topology of energy flows, and the components of the interconnection matrix are impedance which are mainly representations of connected electromagnetic fields. The expression in a general form showing below,

$$\mathbf{L}_W = \mathbf{M}\mathbf{L}^{-1}\mathbf{M}^T = \sqrt{\mathbf{C}}\hat{\mathbf{M}}\hat{\mathbf{M}}^T\sqrt{\mathbf{C}}, \tag{2.33}$$

where,

$$(\hat{\mathbf{M}}\hat{\mathbf{M}}^T)_{kl} = \frac{1}{\sqrt{C_k C_l}} \sum_{m=1}^{n_L} \frac{d_{k\hat{m}} d_{l\hat{m}}}{L_{\hat{m}}}, \tag{2.34}$$

which are the impedance of transmission line or branches.

According to port-Hamiltonian formulism. Eq. (2.31) is network representation of power grid models, which also serves as the topology foundation of complex network models for most of power system analysis.

It clearly suggests that the system structure is an important factor and plays an important role in electric power system, by which to formalize the basic interconnection laws together with the power-conserving elements. That is the basic starting point in the theory of port-Hamiltonian system.

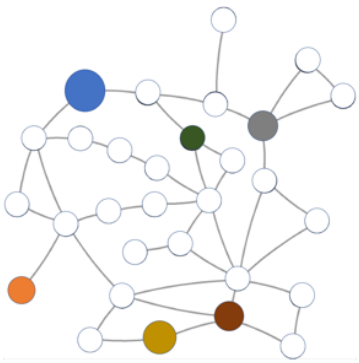

Fig. 2.5: Network representation of the classic electric power system with heterogeneous distribution of generator moment of inertia denoted by different colors.

The advantage of port-Hamiltonian formulism is that it allows us to combine the various dynamic models of all components or subsystems with different physics into an uniform mathematical representation using energy-preserving addition principles.

The above port-Hamiltonian is a representation of a system with single component. For a system with multiple components that interact with each other, the representation for all the components can be easily found because the formulism is based on energy interaction and energy is adaptive. A power system in general comprises of

multiple components which can be presented in terms of interconnection of different port-Hamiltonian systems.

Considering an interconnection of multiple energy systems, its dynamics is given by,

$$\begin{aligned} \dot{x_i} &= (J_i(x_i) - R_i(x_i))\nabla H_i(x_i) + g_i(x_i)u_i + e_i(x_i)v_i \\ y_i &= g_i(x_i)^T \nabla H_i(x_i), i = 1, 2. \end{aligned} \tag{2.35}$$

The simplest illustration, being an interconnection of two port-Hamiltonian system, is shown in Fig. 2.7.

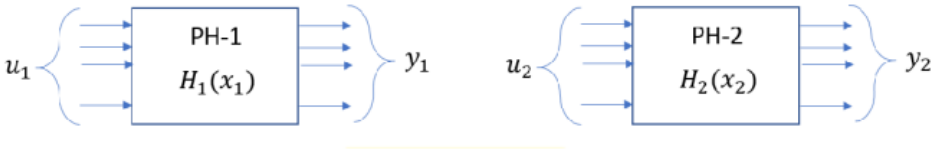

Fig. 2.6: Interconnection of two port-Hamiltonian systems.

Considering port-Hamiltonian representation of two components in a system as shown in Fig. 2.7, we discuss the interconnection of the two components and observe the overall port-Hamiltonian representation. The port-Hamiltonian representation of the two components are shown in Eq. (2.36) and Eq. (2.37),

$$\begin{aligned} \dot{x_1} &= (J_1(x_1) - R_1(x_1))\nabla H_1(x_1) + g_1(x_1)u_1 + e_1(x_1)v_1, \\ y_1 &= g_1(x_1)^T \nabla H_1(x_1), \end{aligned} \tag{2.36}$$

$$\begin{aligned} \dot{x_2} &= (J_2(x_2) - R_2(x_2))\nabla H_2(x_2) + g_2(x_2)u_2 + e_2(x_2)v_2, \\ y_2 &= g_2(x_2)^T \nabla H_2(x_2). \end{aligned} \tag{2.37}$$

If we know the connection structure, say $y_1 = u_2$ and $u_1 = -y_2$, from the above equations, we can derive the overall port-Hamiltonian representation of the system where the overall Hamiltonian function $H(x_1, x_2)$ can be easily obtained as the sum of two

individual Hamiltonian functions shown in Eq. (2.36) i.e. $H_1(x_1) + H_2(x_2)$. Therefore, the Hamiltonian representation of the overall system can be expressed as below,

$$\begin{bmatrix} \dot{x}_1 \\ \dot{x}_2 \end{bmatrix} = (J(x_1, x_2) - R(x_1, x_2))\nabla H(x_1, x_2) + E(x_1, x_2)v, \tag{2.38}$$

where $J(x_1, x_2)$ can be defined as

$$J(x_1, x_2) = \begin{bmatrix} J_1(x_1) & -g_1(x_1)g_2(x_2)^T \\ g_2(x_2)g_1(x_1)^T & J_2(x_2) \end{bmatrix}^T. \tag{2.39}$$

Based on the above example of interconnection of two components in a system, the port-Hamiltonian shows that,

- the system of components has identical forms,
- time domain dynamics (described by right hand side of port-Hamiltonian framework equations) is characterized by J-matrix shown in (2.39).

The port-Hamiltonian of interconnection consisting of a finite number of energy systems can be created in the same way mathematically. No matter how many subsystems are interconnected, the port-Hamiltonian equation of the total system has the same mathematical form as those of individual systems. The illustration of an interconnection of port-Hamiltonian system is shown in Fig. 2.7. Port-Hamiltonian of the power system can be found in a number of literature recently published.

The dynamics of electrical network defined in Eq. (2.31) presents different states associated with the weight, and is comparable to the functional forms of power system models defined using simplified DC power flow as shown in Eq. (2.28). Therefore, we can observe an underlying similarity of port-Hamiltonian representation and its dependence on the network structure with respect to the circuit based representation under various assumptions and conditions.

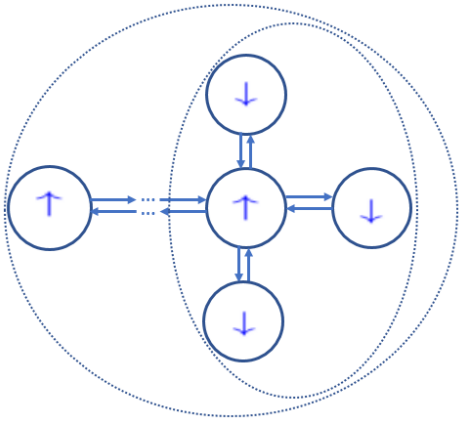

Fig. 2.7: Interconnection of port-Hamiltonian systems.

Eqs. (2.28) and (2.31) are the representation of the power system based on the electric circuit theory under conventional interpretation, i.e., the currents or power flows flow through the power system that are deterministic under KCL and KVL.

Note that port-Hamiltonian formulism can be applied to almost all problems of power system dynamics stability analysis. Thus, the modularity due to the uniformed modeling make it easy to construct explicit global energy or energy-like functions to represent complicated multi-physics interconnections without model approximations and reduction. Port-Hamiltonian formulism has proven highly efficient in modeling and often found usefully in stability analysis and controller designs, such as construction of Lyapunov function for a non-linear multi-physics system. In structural analysis, rather than analyzing the energy function or the characteristics of the complete set of DEAs, the goal is to extract only the topological information embedded in the formulism in stability analysis.

2.2.2 Embeddiy of structural information and applicability

Port-Hamiltonian formulism embeds the structural information. As shown in Equations (2.31) and (2.39), J matrices are derived from the topological structure of interconnection of sub-systems in a network, which naturally contain the embedding of some structural information which represents the network structure.

The uniformity and energy additivity in port-Hamiltonian formulism allow one to define the Hamiltonian of a multi-physics systems with algebraic relations in an identical form [46]. In fact, any power-conserving interconnection of port-Hamiltonian systems again defines a port-Hamiltonian system. Specifically as shown in Equations (2.31) and (2.39), **J-** and $J(\cdot)-$matrices are derived from the topological structure of interconnection of sub-systems in a network, which naturally contain the embedding of some structural information. Significant, possibly dominating, impact of network structure on the dynamical properties of large-scale networks suggests an potential application of Dirac structure, graph and algebraic theories in analyses.

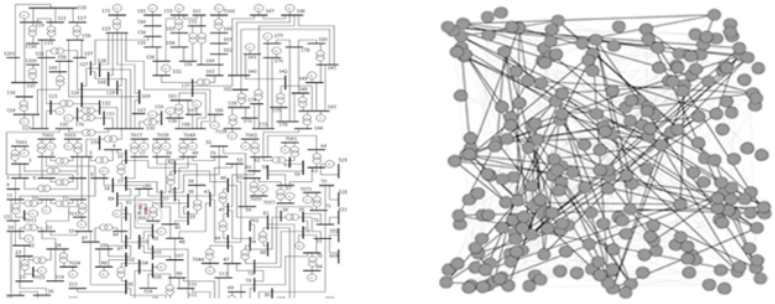

(a) One-line diagram of power grid (b) Topological graph

Fig. 2.8: Topological graph of one-line diagram of power grid.

The structural information includes the topological interconnection data in **J-** and $J(\cdot)-$matrices. For example, a direct transformation of one line diagram to a simple topology graph is shown with plots (a) and (b) in Fig 2.8. The topology of interconnection is represented with various graphs and matrices such as adjacency matrix and Laplacian matrix discussed in the last section.

From the port-Hamiltonian formalism, it is clear to the Laplacian not only exhibits a weighted graph which allows application of complex network theory in some complex problems of power system analysis, more importantly, it reveals the nature of the weights of the Laplacian from an electric circuit perspective.

Many studies, including our early works, were trying to obtain the network properties by analyzing various electric distances based on weighted graphs, constructed by

combining topological graphs and transmission system impedances. Our later research suggested that the applicability of simple weighted graph is very limited in terms provide useful information and additional insights for real problems in practical operations. Therefore, the topological information described by weighted matrices need be modified or corrected for a better representation of network interconnection.

Let's postulate the generalized graph representation for electric power distribution grid. From power perspective, distribution networks modeled as graph, where vertexes represent the buses and transformer of the distribution network, the edges represent the distribution lines. The graph representation of network contains weights. Here, we define 4 kinds of Laplacian matrices for generalized graph representation of distribution network.

Definition of L_W: In the real power distribution system, considering the line impedance, that is if $Z^{-1} \neq aI$ and $\Psi^{\dagger}$=b(I-$\mathbf{1}_0\mathbf{1}_0^T$), we define the weighted Laplacian matrix written as $(L_W)_{N\times N}$:

$$(L_W)_{N\times N} = F_{M\times N}^T Z^{-1} F_{M\times N}, \tag{2.40}$$

where $F_{M\times N}$ stands for the incidence matrix of graph G, and $\mathbf{Z}$ is the diagonal matrix of the line impedances;

Definition of L_Ψ: In the real power distribution system, considering the injection power on each nodes, that is if $Z^{-1} = aI$ and $\Psi^{\dagger} \neq$ b(I-$\mathbf{1}_0\mathbf{1}_0^T$), where a and b are constants, we define the Laplacian matrix written as $(L_\Psi)_{N\times N}$:

$$(L_\Psi)_{N\times N} = (L_{N\times N})\Psi^{\dagger}(L_{N\times N}). \tag{2.41}$$

Definition of $(L_{W\Psi})_{N\times N}$: Considering the line impedance and injection power on each nodes in the real power system, that is if $Z^{-1} \neq aI$ and $\Psi^{\dagger} \neq$ b(I-$\mathbf{1}_0\mathbf{1}_0^T$), we define the

Laplacian matrix written as $(L_{W\Psi})_{N\times N}$, and we define $\mathcal{L}_{=}L_{W\Psi}$

$$(L_{W\Psi})_{N\times N} = (F^T Z^{-1} F)\Psi^{\dagger}(F^T Z^{-1} F). \tag{2.42}$$

Comparing the existing graph representation, the definition with Eq. (2.42) is a more general graph representation of power grids: it not only includes commonly used $L_{N\times N}$ and $(L_W)_{N\times N}$, it also integrates the information of power injections. Therefore, $(L_{W\Psi})_{N\times N}$ is conceived as a generalized graph representation of the power grid.

Remarks:

From the port-Hamiltonian formalism, it is clear to the Laplacian not only exhibits a weighted graph which allows application of complex network theory in some complex problems of power system analysis, more importantly, it reveals the nature of the weights of the Laplacian from an electric circuit perspective.

Particularly, as suggested in a further investigation [47], it is showed that weights of Laplacian matrices themselves are critical quantities that characterize some important dynamics in power system analysis and are the building blocks to defineso-called *electric distance* used to quantify sensitivities used in power engineering community. Electric distance can be component inductance such as transmission line inductance, electric machine coupling inductance in simple cases because of its similarity of the geometric distance from a topological view, or their linear transformations of component inductance representing other types of sensitivity in analyses of more complicated problems. For different problems, different types of electric distance are constructed. More interestingly, since there is only physical power grid, different interconnection matrices thus representation of subjective views or modifications of an objective presence.

Electric distances 1) serves as graph distance of under various topological connection based on classic complex networks theory or electric distances various circuits based on electric engineering theory which suggests some possible unified view about energy

transient on the power grid, which previously interested separately in power engineering, network science and physics; 2) illustrates that weights of the Laplacian of a lossless grid are reactance of transmission lines, linear representation of interconnected electric fields and magnetic fields; 3) it unifies circuit impedance, electric distance and graph distance. electromagnetic fields in physics.

Consideration of entries in the Laplacian as distances goes beyond the provision of edge weights of topological connection. Having a notion of distance that is built on the circuit sensitivities representing the coupling interactions among interconnected electric fields and magnetic fields, which at the same time is interpreted with respect to the ubiquitous proprieties of complex networks, highlights the importance of distance from power system engineering (electric distance), complex network theory (graph/resistance distance) and physics (state of interacting electric and magnetic fields).

This distance view highlights the limitation of direct transformation of an electric-circuit based model to its graph representation in power flow analysis. Knowing that electric-circuit based models of power flow mathematically are a set of frequency domain functions built on the fundamental frequency waveform component (@50/60Hz). This cycle-based models for H in Eq. (4.10) is the base for all other components including the harmonics, symmetrical components and noises, thus both resolution of original impedance-based electric circuit models and predictability of the distance-based network properties are defined by the accuracy of impedance in one cycle time frame of the fundamental frequency.

In other words, the fundamental frequency component based family of frequency domain models of power system analysis required at least cycle-long validation. Therefore, electric circuit based models are accurate in a longer time horizon, while less accurate during the transient period, particularly the sub-transient period.

Theoretically, simple scale-free applicability of the network-based models or methods is inadequate for description of energy flow during sub-transient period such as those

in cascading failures, because "graph distance" in a small-world complex network does not have the flexibility of adding additional frequency components of its electric circuit original, nor its connectivity provide additional information that the original model does have.

CHAPTER 3

A Hypothetical View on Energy Flow in Power Grid

Inspired from the existing works, in this chapter, a integrated hypothetical view on energy flow in power grid is postulated. Here the power grid refers to the transmission system in electric power system. The hypothetical view comes from three inspirations. Let's talk about the inspirations first.

3.1 Inspirations from the investigation of recent works

Some prior investigations on the nature of connections between the structural properties of electric power grid and the characteristics of energy flow highlighted several interesting observations.

The integrated power grid hypothetical view is inspired from three observations based on some recent investigations on structural and functional properties related to the attributes of links in power system models : 1) unification of power system models under the port-Hamiltonian formalism, 2) application of advanced structural analysis, and 3) reformulation of a fundamental general power flow model into probabilistic random-walk representation on graph of power flow models.

3.1.1 A physics interpretation of port-Hamiltonian representation

The first inspiration comes from a physics interpretation of port-Hamiltonian representation of power grid. The observation on the Laplacian matrix of power system model suggests the physics nature of power grid that it is a manifestation of interconnected electromagnetic field.

It is known that, a network model of power system analysis can be uniformly representation with the port-Hamiltonian formulism [38, 47]. Port-Hamiltonian formulism is a network representation of power grid models, which also serves as the topology foundation of complex network models for most of power system analysis. The result interconnection Laplacian matrix can be seen as a weighted graph that explicitly represents the topology of energy flows, and the components of the interconnection matrix are impedance which are mainly representations of connected electromagnetic fields. These impedances sometimes are called electric distance. For different problems, different types of electric distance are constructed. More interestingly, since there is only physical power grid, different interconnection matrices thus are representations of subjective views or modifications of an objective presence.

Port-Hamiltonian formalism is a system engineering modeling approach for dynamical analysis of nonlinear multi-physics systems [38]. As summarized in [43], almost all power system models can be rewritten using port-Hamiltonian formalism [38, 47], with characterizing Laplacian matrix, including the governing $\mathbf{H}$ pertinent to the models and functions governing energy influx in Eq. (4.10) (shown in next chapter). $[\dot{q(t)}, \dot{\varphi(t)}] = = [0\ \mathbf{M}, -\mathbf{M}^T\ 0][C^{-1}q(t), L^{-1}\varphi(t)]$, where $q(t) \in \mathbb{R}^{n_C}$ and $\varphi(t) \in \mathbb{R}^{n_L}$ are vectors of capacitor charges and inductor fluxes at time t respectively. $C = \mathrm{diag}(C_1 \cdots C_{n_C})$, $L = = \mathrm{diag}(L_1 \cdots L_{n_L})$, C_i is the capacitance of the i^{th} capacitor, and L_j is the inductance of the j^{th} inductor. $\mathbf{M}$ is the incidence matrix of represented network of electric power system. The characterizing Laplacian matrices of port-Hamiltonian system can be seen as a weighted graph that explicitly represents the topology of energy flow

$$\mathbf{L}_W = \mathbf{M}\mathbf{L}^{-1}\mathbf{M}^T = \sqrt{C}\hat{\mathbf{M}}\hat{\mathbf{M}}^T\sqrt{C}, \tag{3.1}$$

and the components of the interconnection matrix are Laplacian matrices. And the Laplacian matrices essentially are impedance matrix which are mainly representations

of an interconnected electromagnetic fields

$$(\hat{\mathbf{M}}\hat{\mathbf{M}}^T)_{kl} = \frac{1}{\sqrt{C_k C_l}} \sum_{m=1}^{n_L} \frac{d_{k\hat{m}} d_{l\hat{m}}}{L_{\hat{m}}}. \tag{3.2}$$

According to port-Hamiltonian formulism, Eq. (3.1) is network representation of power grid models,which also serves as the topology foundation of complex network models for most of power system analysis.

This observation on the Laplacian of power system model suggests the physics nature that is an unitary electromagnetic field view underlying engineering power system models, their graph representations under physics, and unifies the electric distance in power system engineering, graph distance [48] in complex networks, and coupling strength of electromagnetic fields in physics.

3.1.2 Practical network structural analysis

The second inspiration comes from an example of structural analysis that is restoration evidential application. Application of structure analysis suggest the network structure has an important, even dominating, impact on dynamic stability of power grid. As shown in the example of evidential application of system restoration [49], using structure information can quickly find critical or most effective paths that have less the stability issues as shown in Fig. 3.1 [47, 50].

In structural analysis, rather than analyzing the energy function or the characteristics of the complete set of DEAs, the goal is to extract only the topological information embedded in the formulism in stability analysis.

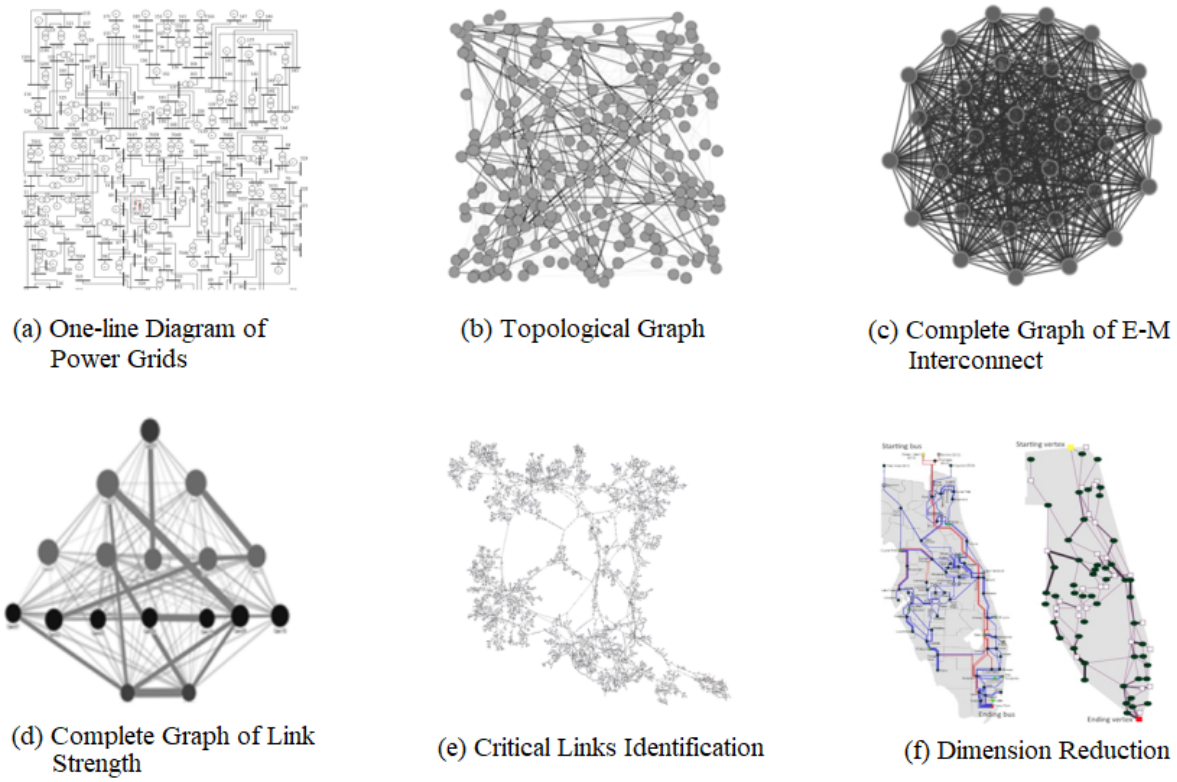

Fig. 3.1: Illustration of solution space reduction.

3.1.3 Random-walk-on-graph perspective of network power flow

The third inspiration comes from an implication of random-walk-on-graph. One of recent work proof that, mathematically, power flow model can be converted to a random walk model [51, 52]. The observation on random-walk-on-graph related work suggests a dramatic new interpretation of energy flow in power grid, which is different from a classic or small world perspective that the electric power grid is considered as a delocalized system of energy. which suggest power system can be seen as a delocalized system.

Some recent works seek new network properties that characterizing the structural complexities of real world networks. Random walk on general network and graph/resistance distance have been discussed in mathematics community [53, 54, 55].

Specifically, the power grid can also be conceived as an one-world. For example, particularly, in [51], it was found that a fundamental power flow model can be precisely transformed into a probabilistic random walk on graph representation. In this model,

the power flow can be seen as random power flows on a complete graph with a probability function that depends on the associated electric distances. And the resultant node or bus angle of the power grid , which governs the energy flow over transmission lines, corresponds to a probabilistic state involving simultaneous and random energy flows between all pairs of nodes as if they are connected through a complete graph. The arriving probabilistic distribution are characterized by the interconnection Laplacian weights or electric distances described in Laplacian interconnection matrix and its inverse.

An potential application of the concept described in [51] that applying the random walk concept and graph distance to estimation of energy flow was successfully demonstrated through an experiment with a toy power system model with 49-generators interconnected through lattice graph and homogeneous inertia distribution [21].

It is also shown that the probability distribution of state transitions is typically represented as the fundamental Markov chain's transition matrix [53, 54, 55], which can be constructed based on the Laplacian and its inversion using the method showing in [55]. The effective electric distance used to calculate the Markov chain [53, 54, 55] that represents the system states (the power angle) depends on the connectivity of all pairs of vertices as if the grid follows a complete graph representation. Such relationship between the probabilities of the transition matrix and graph/resistance distance associated with complete graph are also discussed in mathematics community in [53, 54, 55]. In the case of connected graphs, the generalized inverse of the Laplacian matrix can be expressed in terms of the resistance matrix to represent the link strength that depends on all pairs of vertices.

The important concepts in random-walk-on-graph representation of power flow equations can be illustrated by an conceptual application that is port energy automaton [21] as shown in Fig. 3.2. Port energy automaton is designed with the condition of complete graph representation. Under this assumption, the same energy flow characteristics were obtained with other methods.

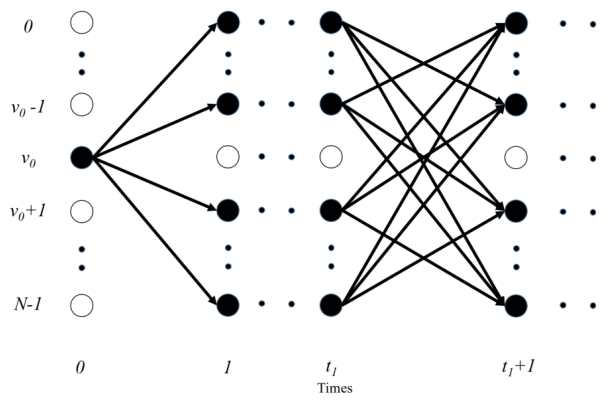

Fig. 3.2: Energy flow in the network.

3.1.4 Remarks

The aforementioned observations have been mentioned in some other literature, which gave raise to some fundamentals due to the intrinsic limitation associated with the cycle-resolution of graph weight or graph distance. Are complex networks models and proprieties are truly scale-free to interpret transients in real world complex network? Due to the complex nature of power flow in a transient period, can we use static structural information to predict the power flow during a transient period? Although any known waveform can be replicated accurately with a set of frequency domain sinusoidals, what if the complex power flow during the transient period tends to follow the Heisenberg uncertainty principle in terms of time and energy (i.e., $\Delta E \Delta t \approx Constant$), is it still predictable?

The three observations on some recent works in engineering and mathematics perspectives gave rise to a new physics view of power grid as a unitary electromagnetic field.

Motivated by the difficulties associated with the unclear nature of the uncertainties of energy flow during transient periods, the progress is made on one-world interpretation of a random walk representation of a fundamental power flow model e.g. in [51], and the fact that the electric power grid is an synchronized complex network linked with synchronized or coherent electric-magnetic fields. It is natural to exploit answers from physics theory and methods, to see if the modern physics theory and methods support

the one-world or complete graph representation of power grid and to find new network properties to address some real world transient problems.

To obtain the maximum flexibility of bearing quantum theory and methods on energy transient problems, we would like to the following hypothetical view based on our prior research and experience, particularly those related to one-world mathematical representation of power grid having complete coherence links between all pairs of nodes.

3.2 New wave-based view on power system electro-mechanical dynamics

Based on the inspirations in section 3.1, the power system dynamics can be considered from the wave perspective.

The dynamics stability of synchronous machines in electric power system can be determined by the swing equation as follows,

$$M\frac{d^2\delta}{dt^2} = P_m - P_e, \tag{3.3}$$

where, M represents the angular momentum of the machine, δ is the angular displacement, and P_m and P_e are the mechanical power input and electrical power output, respectively. For a uniform one-dimensional chain discrete power system using the distributed parameters $y^{'}$, $m^{'}$ and $k^{'}$ that the line reactance $X = xl$, inverse of machine reactance $Y = y^{'}l$, the machine inertia $M = m^{'}l$ which is proportional to its size, the distance between buses l, and the defining transmission capacity for lossless lines $K = \frac{V^2}{X} = \frac{k^{'}}{l}$, the swing equation can be considered from the wave perspective as follows,

$$\frac{\partial^2\xi}{\partial x^2} = \frac{m^{'}}{k^{'}}\frac{\partial^2\xi}{\partial t^2}, \tag{3.4}$$

The second order linear differential Eq. (3.4) of lossless one-dimensional propagation is considered as the of electro-mechanical dynamic equation of electrical power system

from the wave perspective. In Eq. (3.4), ξ can be angular displacement δ, angular velocity ω and power P.

3.3 Postulation of hypothetical view on energy flow in power grid

Above observations, new explorations, thinking and wave-based view in section 3.1 and 3.2 give rises to a conjunctive view on electric power grid as a delocalized system of energy, hence naturally motives us to switch from the classic small-world network perception to a new one of on-world network, aiming at seeking tools from fundamental physics.

3.3.1 Description of hypothetical unitary field view

Based on the inspirations, insight and understanding of the investigation results, the integrated power grid hypothetical view is postulated, which includes the following hypothesises.

H1 Delocalized many-body system of energy

- A unitary field
- A complete graph

H2 Particle-wave property of energy exchange at ports (generation and load nodes, etc.)

H3 Relativistic time-space view

3.3.1.1 Delocalized many-body system of energy

In the complex electric power system network with multi-ports, the whole system is considered as a delocalization of many-body system. The many-body energy system

is constituted with many different elementary-unit-like particles. In general, every elementary-unit-like particle is treated as interacting with all the other elementary-unit-like particles. Any elementary-unit-like particle is simultaneously associated with all other elementary-unit-like particles in many-body system representing the electric power system network, and we can not just consider each elementary-unit-like particle itself and adjacent ones connected physically at a time. Any elementary-unit-like particle behavior extends over the whole system framework. The delocality indicates that there exists a correlation among elementary-unit-like particles. Also, the unitary view with homogeneity is considered so that physics can be applied.

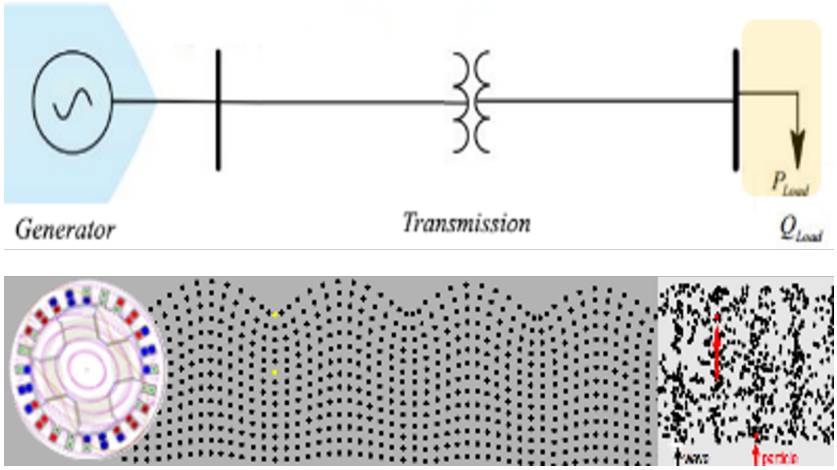

Fig. 3.3: Propagating electromagnetic field in the simple electric power system.

A unitary electromagnetic field:

From the fundamental physics perspective, the electric power grid is a unified electromagnetic field of rigid body constituted by n particles essentially. And the behavior of the system is determined by such a electromagnetic field, which can be shown using a simple two ports electric power system shown in Fig 3.3.

A complete graph:

Knowing the power grid is a network of energy systems that are synchronously linked through eclectic and magnetic field, the aforementioned investigation and observations suggested some possible hidden linkages between the dynamics of energy flow and ef-

fective electric distance, which might be difficult to discover with classic electric circuit theory-based analytics and complex network theory. For example, the effective electric distance used to calculate the Markov chain that represents the system states (the power angle) depends on the connectivities of all pairs of vertices as if the grid follows a complete graph representation.

In power grid dynamic structure analysis, in addition to using information interconnection represented by weighted topological graph, it is also critical to look at the interconnection from the flip-side, that considering the graph as a complete graph [56]. The network representation is fully connected network that each port connects with all other ports. As shown in Fig. 3.4(a), a complete graph contains some important information about the linking strengths described by lumped-parameters from a global perspective.

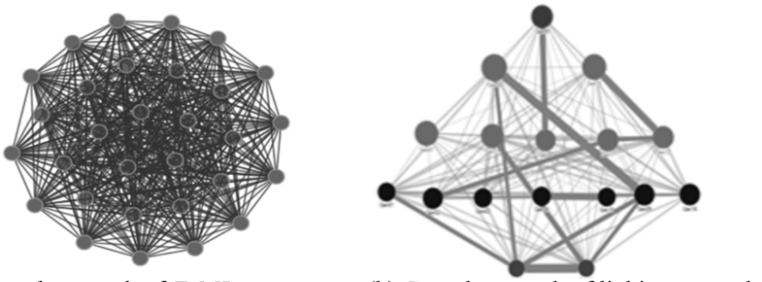

(a) Complete graph of *E-M* Interconnect (b) Complete graph of linking strength

Fig. 3.4: Complete graph representation.

The complete graph representation also includes the heterogeneity of the power grid in terms of inertia constants and nodal powers. As shown in Fig. 3.4(b), in additional to graph weights from transmission system impedances, information such as the differences among nodal inertia constants and nodal powers need to be appropriately taken into consideration as additional layers of information in terms of system heterogeneity. These additional layers of information have significant impact on the network properties thus should be included in correction or modification of the original weight topological graph as discussed in section 2.2.2.

The complete graph representation of power grid can be illustrated using a quantum

magnetosphere, which is very important to understand the interaction of energy and information of the system. The network representation of the electric power system is considered as a complete network. Each pair of distinct network nodes is connected by a unique linking, which can be illustrated in Fig. 3.5. The top operator layer is the real

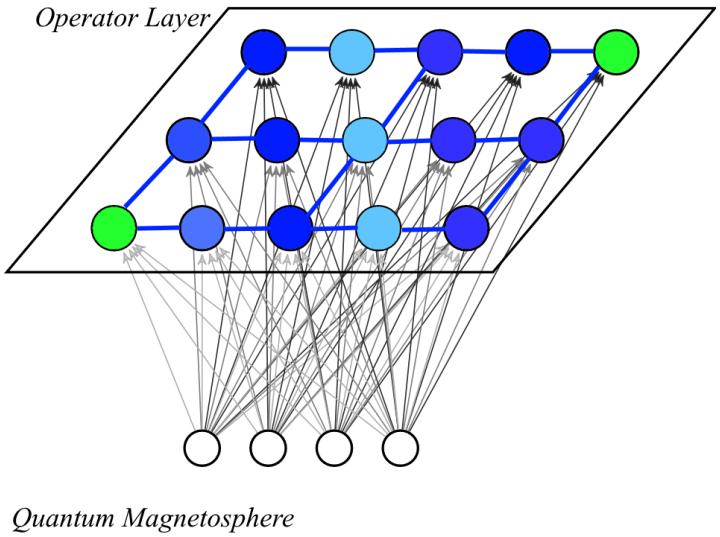

Fig. 3.5: Quantum magnetosphere.

physical connection structure. It is one of the observation layers with certain probability. It is a further description or transformation mathematically without changing the real physical connection structure, which corresponds the $\mathscr{L}_{W\Phi}$ we discussed in section 2.2.2. Every port can be seen as a spin model. Different colors of them represent the different spin angles. Here, the color changing is very fast, which forms a certain pattern overall corresponding to the quantum state or electric current. Different layers with different kinds of colors in the top represents the different quantum states essentially. The time evolution of the pattern can be represented by the left-hand-side (LHS) of Schrödinger equation. Each port in the quantum magnetosphere represents the generator. The bottom layer is a fundamental change of state and represents the complete structure, which is considered as a physics existence. Between the top and bottom layer, there exists a pattern.

3.3.1.2 Particle-wave property of energy exchange at ports

The second hypothesis is about the nodes in power grid. The energy exchange of generation nodes and load nodes have similar particle-wave property. The ports in power grid can be generate energy or withdraw energy and the energy exchanges on the nodes has particle-wave property. For one hand, waves exhibit particle-like characteristics,

$$\begin{aligned} E &= h\nu = \hbar\omega, \\ \vec{p} &= \frac{h}{\lambda} = \hbar\vec{k}. \end{aligned} \tag{3.5}$$

For the other hand, Particles behave like waves and exhibit interference effects. The wavelength of a particle is derived as following equation,

$$\lambda_w = \frac{h}{m_p v} = \frac{h}{p}, \tag{3.6}$$

where, E is the energy of the particle, $\vec{p}$ is the momentum of the particle, m_p is the particle mass (in kilograms), and v is the traveling velocity (in m/s). h is the Planck's constant ($6.626 \times 10^{-34} kg \cdot m^2/s$), $\hbar$ is the reduced Planck's constant, $\vec{k}$ is the wave vector, λ_w is the de Broglie wave length of the particle in metres, and ω is the angular frequency, and ν is the vibration frequency of the particle.

3.3.1.3 Relativistic time-space view

The third hypothesis is a relativistic time-space view of the energy flow propagation and time domain variation of particles. We consider spatial propagation of energy is slower than the time domain variation of particles. Time domain variation of particle movement is fast, while the result of movement is slow. Even in a short time period, multiple movement processes have completed.

In the unitary electromagnetic field, the energy flow characteristics can be described by electromagnetic wave from two separate perspectives: time-domain variation of the

magnitude of transverse wave at each spot of the delocalized energy system and propagation of electromagnetic wave along z-direction longitudinally. Electromagnetic wave propagates as a result of time-domain variation of 2-dimensional alternating transverse waves at each spot of the system. The energy flow defined along the z-direction is conceived as spatial energy propagation driven by electric and magnetic waves transverse plane ($x-y$ plane). We consider there exists a relativistic time-space relationship between the spatial energy propagation in the z-direction and the time domain variation in the transverse plane of electromagnetic wave.

3.3.2 Illustration of the hypothetical view

The electric power system is considered as one unified field, i.e.,a interconnected electromagnetic field essentially. The characteristics of fully connected electric power system network is determined by the boundary-field (B-F) and neighboring-field (N-F). B-F corresponds the delocalized quantum state behavior of the elementary-unit-like particles (magnet dipoles considered). N-F only indicates the relationship between ports and their close neighbors.

The interconnected electromagnetic field view from the classic perspective can be represented by the following matrix illustratively,

$$H_{complete}^{classic} = \begin{bmatrix} H_{11} & H_{12} & \cdots & H_{1n} \\ H_{21} & H_{22} & \cdots & H_{2n} \\ \vdots & \vdots & \vdots & \vdots \\ H_{n1} & H_{n2} & \cdots & H_{nn} \end{bmatrix}. \tag{3.7}$$

Interconnected electromagnetic field is driven by B-F and N-F with n entangled particles or superposition eigen-states,

$$\hat{H}_{complete}^{quantum} = \hat{H}_k \oplus \hat{H}_{ij}, \tag{3.8}$$

where $\hat{H}_k$ is the B-F operator and $\hat{H}_{ij}$ is the N-F operator. The variation of the movement of particles is the joint effect of B-F and N-F.

From the quantum perspective (complete graph representation perspective), interconnected electromagnetic field view can be generalized by the Hamiltonian operator $\hat{H}^{quantum}_{complete}$ as follows,

$$\hat{H}^{quantum}_{complete} = \begin{bmatrix} \hat{H}_{11} & \hat{H}_{12} & \cdots & \hat{H}_{1n} \\ \hat{H}_{21} & \hat{H}_{22} & \cdots & \hat{H}_{2n} \\ \vdots & \vdots & \ddots & \vdots \\ \hat{H}_{n1} & \hat{H}_{n2} & \cdots & \hat{H}_{nn} \end{bmatrix} = \tag{3.9}$$

$$\begin{bmatrix} \begin{bmatrix} \kappa^{11}_{11} \cdots \kappa^{11}_{1n} \\ \vdots \ddots \vdots \\ \kappa^{11}_{n1} \cdots \kappa^{11}_{nn} \end{bmatrix}_{11} & \begin{bmatrix} \kappa^{12}_{11} \cdots \kappa^{12}_{1n} \\ \vdots \ddots \vdots \\ \kappa^{12}_{n1} \cdots \kappa^{12}_{nn} \end{bmatrix}_{12} & \cdots & \begin{bmatrix} \kappa^{1N}_{11} \cdots \kappa^{1n}_{1n} \\ \vdots \ddots \vdots \\ \kappa^{1n}_{n1} \cdots \kappa^{1n}_{nn} \end{bmatrix}_{1n} \\ \begin{bmatrix} \kappa^{21}_{11} \cdots \kappa^{21}_{1n} \\ \vdots \ddots \vdots \\ \kappa^{21}_{n1} \cdots \kappa^{21}_{nn} \end{bmatrix}_{21} & \begin{bmatrix} \kappa^{22}_{11} \cdots \kappa^{22}_{1n} \\ \vdots \ddots \vdots \\ \kappa^{22}_{n1} \cdots \kappa^{22}_{nn} \end{bmatrix}_{22} & \cdots & \begin{bmatrix} \kappa^{2n}_{11} \cdots \kappa^{2n}_{1n} \\ \vdots \ddots \vdots \\ \kappa^{2n}_{n1} \cdots \kappa^{2n}_{nn} \end{bmatrix}_{2n} \\ \vdots & \vdots & \ddots & \vdots \\ \begin{bmatrix} \kappa^{n1}_{11} \cdots \kappa^{n1}_{1n} \\ \vdots \ddots \vdots \\ \kappa^{n1}_{n1} \cdots \kappa^{n1}_{nn} \end{bmatrix}_{N1} & \begin{bmatrix} \kappa^{n2}_{11} \cdots \kappa^{n2}_{1n} \\ \vdots \ddots \vdots \\ \kappa^{n2}_{n1} \cdots \kappa^{n2}_{nn} \end{bmatrix}_{n2} & \cdots & \begin{bmatrix} \kappa^{nn}_{11} \cdots \kappa^{nn}_{1n} \\ \vdots \ddots \vdots \\ \kappa^{nn}_{n1} \cdots \kappa^{nn}_{nn} \end{bmatrix}_{nn} \end{bmatrix}$$

. The Hamiltonian operator $\hat{H}_k$ for B-F can be generalized as,

$$\hat{H}_k = \begin{bmatrix} h^k_{11} & h^k_{12} & h^k_{13} & \cdots & h^k_{1m} \\ h^k_{21} & h^k_{22} & h^k_{23} & \cdots & h^k_{2m} \\ \vdots & \vdots & \vdots & \ddots & \vdots \\ h^k_{m1} & h^k_{m2} & h^k_{m3} & \cdots & h^k_{mm} \end{bmatrix}, \tag{3.10}$$

and the Hamiltonian operator $\hat{H}_{ij}$ for N-F can be generalized as,

$$\hat{H}_{ij}=\begin{bmatrix} \kappa_{11} & \kappa_{12} & \kappa_{13} & \cdots & \kappa_{1N} \\ \kappa_{21} & \kappa_{22} & \kappa_{23} & \cdots & \kappa_{21} \\ \vdots & \vdots & \vdots & \ddots & \vdots \\ \kappa_{N1} & \kappa_{N2} & \kappa_{N3} & \cdots & \kappa_{NN} \end{bmatrix}_{ij} . \tag{3.11}$$

The views of B-F and N-F is as follows.

- B-F determines the the coordinate of each port.
- N-F determines the interaction between ports.
- N-F is influenced by the B-F.
- N-F considers the effect of the link strength between ports and the power of each port.
- In the electric power system, if any port is effected by the external B-F operation, any other ports will be influenced immediately.
- B-F is taken as a physical entity simultaneously distributing in space. Based on Maxwell's equations, it is considered that B-F transmits with fast speed and are perceptive by particles simultaneous.
- B-F corresponds the radiation of the accelerating spins with fast speed.
- While, the ergodic motion of a particle exists throughout N-F space in an essentially local way. The particle is still in one position at each instant, and it is only during a time interval that the ergodic motion of the particle spreads throughout space.
- In the N-F operation area, electromagnetic wave propagates through the media.

- The transmission of B-F is fast (information transmission), while the variation of B-F is slow. B-F is related with energy. The variation of energy is slow and it needs time.

- B-F defines the whole space-time. N-F is considered as the instantaneous perceptions of magnetic field.

- B-F is considered as radiation field. N-F is the result of the charge and rotational movement of the elementary-unit-like particle and is considered as induction field.

- N-F is considered as the relativistic effect of the B-F.

- N-F is derived by B-F, which needs to be understood through unified four dimensional electromagnetic field tensor. N-F is considered as the spatial component of the four dimensional tensor and B-F is considered as the time component of the four dimensional tensor.

- The existence of B-F must be accompanied by the existence of N-F, which is indicated by the time-space special relativity theory described by Einstein. It can be said that N-F that exists in the macro low-speed world is a powerful proof of the correctness of the relativistic space-time concept.

Connections of B-F and N-F to Schrödinger equations, i.e., corresponding to left-hand-side (LHS) and right-hand-side (RHS) of Schrödinger equation

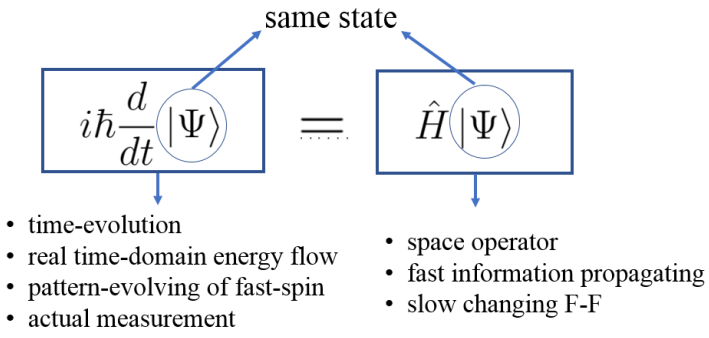

Fig. 3.6: Connections of F-F and N-F to Schrödinger equations.

The connection of B-F and N-F to Schrödinger equations is illustrated in Fig. 3.6

LHS of Schrödinger equation represents the slow pattern-evolving of fast rotational movement, corresponding to real time domain energy flow of interconnected magnetic dipoles or N-F in response to B-F.

RHS of Schrödinger equation corresponds to fast information propagating but slow changing of B-F. B-F is conceived as the fundamental unity that sending information to and received simultaneously by every particle but such an information or operation cannot be quantized or measured in terms of energy because measurement is based on accumulated energy over time. So actual measurement has to be done in the LHS of Schrödinger equation, not the RHS of Schrödinger equation.

However, the Schrödinger equation is about the same quantum "state". Therefore, we can estimate the whole system state through a very short time period (LHS of Schrödinger equation) thought the spatial structure (RHS of Schrödinger equation). It is not necessary to wait a long time.

LHS and RHS of Schrödinger equation address the issues of applying distributed algorithm in protection scheme design, i.e., RHS of Schrödinger equation provides the general reference needed, and LHS of Schrödinger equation adopts distributed algorithm.

Energy flow illustration with B-F and N-F

Energy flow (wave) can be illustrated under the B-F and N-F views.

The rotational movements of elementary-unit-like particle (magnetic dipole model) in interconnected electromagnetic field is the joint effect of B-F and N-F. The rotational movement of an elementary-unit-like particle is influenced by N-F when the B-F is constant. A magnetic field will cause rotational procession of the elementary-unit-like particle, which is around the direction of the magnetic field. Some information is based on the rotational procession rate of the magnet dipoles.

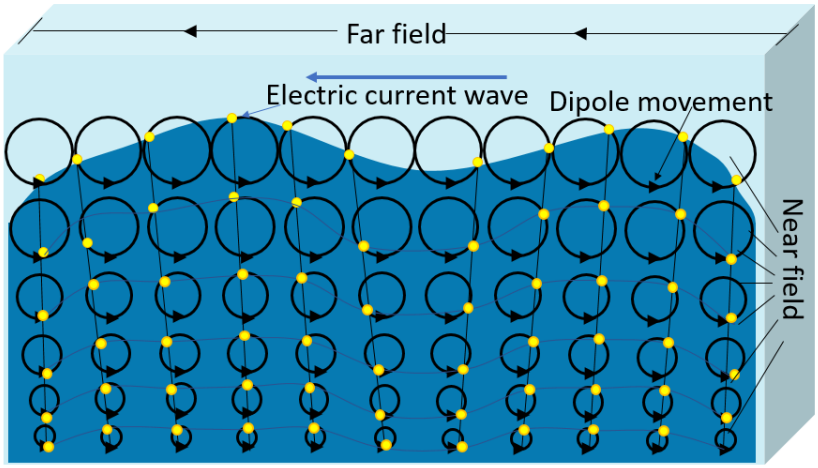

Fig. 3.7: Schematic diagram of energy wave.

The elementary-unit-like particle rotates fast and radiates the wave with fast speed. The statistic average of the movement state of the elementary-unit-like particles forms the energy flow state, which is related with the medium and is another source of the magnetic field. The wave function of the conduction current is travelling wave that constitutes with infinite electromagnetic waves. Energy flow is illusive and can be seen as the effect of the interaction of N-F.

From the macro perspective, these charge carriers and dipoles variation under the field can be seen as a state. Such a state constructs the energy flow or conductive electric current we normally discuss. The schematic diagram of electric current wave is shown in Fig. 3.7.

The variation of the electric current, such as the one during the transit state depends on the property of media. In fact, the microscope conduction current comes from the microscope electron arrangement and interaction patterns inside the media. It can be interpreted by the collective behavior closely related to dipoles movements under the field.

The near field refers to electromagnetic fields near the charges and current, therefore, electric current can be seen as the effect of near field on the media.

3.3.3 Remarks

Above statements have analytical solid foundation, however it is not mature enough to call this as a theory and we call the statements description as a hypothetical view.

However, the postulated hypothetical view is novel in that the hypothetical view of energy flow in power grid is based on physics concepts and principles which are different from the model suggested by electric-circuit theory. Remarks of postulated hypothetical view on interconnected electric power system are as follows.

The delocalization property can be used to understand the underlying causes of steady state of electric power gird. The existence of a stable structure of electric power system is due to the in-distinguish property of identical elementary-unit-like-particles. In electric power system, elementary-unit-like particles no longer belong to a specific port, but they form delocalized particles, such that a new interaction occurs-system linking force. It is the system linking force to combine all the ports together.

The postulated hypothetical view is useful in that the unitary view with homogeneity is considered so that physics can be applied. Specifically, with the quantum effect assumption, the element-unit-like particle with fast rotational movement is considered. Relativistic time-space view is a whole frame of the system, under which the characteristics are realized through quantum principle-Schrödinger equation. The LHS of Schrödinger equation is the time evolution of slow pattern after countless fast rotational movement. The LHS of Schrödinger equation is considered as the space operator applying information that can be perceived simultaneous. In Schrödinger equation, the same entangled state wave function is a complete description of a single elementary-unit-like particle. It is because of the same state, the LHS and RHS are time-space complementary, i.e., space state is derived according to time experimentally, and time evolution state is obtained after space operator.

The proposed hypothetical view provides a completely delocalized picture of the link-

ing in the complex electric power system network, which is capable of explaining and predicting some essential phenomenon in a complex power system network like the stability predictions. Also, the results obtained using this proposed view are generally in good agreement with a large body of experimental data and have given extremely useful insights into the nature of electric power system operations.

This unitary electromagnetic field view may not be completed a new conjecture as there have been discussions and research on Laplacian matrix of connected graphs and the property of its inverse as an completed graph [53, 54]. In the case of connected graphs, the generalized inverse of Laplacian matrix can be used to represent the effective links (referenced to as resistance distance in some literature) between nodes [53, 54]. However, it is still a hypothesis for interpretation of energy transient in synchronous power grid, particularly when we are granting it quantum field properties that has been fully tested and agreed.

Specifically, under the hypothetical view, the particle with fast rotation is considered. Relativistic time-space view is a whole frame of the system, under which the characteristics are realized through quantum principle-Schrödinger equation. The LHS of Schrödinger equation is the time evolution of slow pattern after countless rotation with fast speed. The RHS of Schrödinger equation is considered as the space operator applying information that can be perceived simultaneous. In Schrödinger equation, the same delocalized state wave function is a complete description of a single particle. It is because of the same state, the LHS and RHS are time-space complementary, i.e., space state is derived according to time experimentally, and time evolution state is obtained after space operator.

The integrated electric power grid hypothetical view inspires the curiosity about the nature of energy flow in power grid: what if the sub-transient energy flow does not admit a classical time-space picture or well-defined models that are priori known, in the similar sense in which there is no single time domain trajectory of microscope

particle motion? What if there are fundamental physics effect in the synchronized electric and magnetic fields of power grid? From a fundamental physics perspective, can fundamental physics theory offer more insights on how to quantify the relationship between structural properties of complex networks and dynamics of energy flow in real system? Is the network structural information can really predict the time domain energy transients in real-system? Can we use space domain or structure information to predict time domain propagation of energy with industrial grade accuracy for practical reality application? Can we use featureless modeling to get maximum flexibility to break the limit of cycle-dependent sinusoidal form of frequency domain model?

Note that different from a small-world perspective on power grid, the hypothesis allows us to obtain maximum flexibility to take the advantage of some fundamental principles and tools to break the limit of the cycle-dependent sinusoidal family of frequency domain model. That are not offered or supported by classic physics based electric circuit and solve real world problems. This hypothesis allows us to use first-principles account of a quantum or "quantumic" analytic for understanding some complex behavior of energy flow during transient period. Moreover, it offers more tangible from physics perspective that quantum information theory or models as the power grid indeed an interconnected electromagnetic field.

In the next chapter chapter, I will show that the hypothesis allows us to obtain maximum flexibility to take the advantage of some fundamental principles of tools: to break the limit of the cycle-dependent sinusoidal family of frequency domain model. We are able to use 1)featureless quantum number-based model, and 2) application of Heisenberg uncertainty principle, quantum number-based model, quantum states, tool-operators to derive an unified principles of evolution yielding a different dynamical behavior for microscopic and macroscopic objects. That are not offered or supported by classic physics based electric circuit and solve real world problem.

Postulation of integrated hypothetical view allows us to bear theory and tools from

quantum physics. Specifically, in the following chapter, a new theoretical quantum number-based (n-l-m) model of electric power grid will proposed based on the hypothetical view, extended physics illustration with boundary field and neighboring field, and the experience and knowledge in power grid, which can help to get better understanding of some characteristics of the electric power grid energy flow and to solve some existing complex problems potentially.

CHAPTER 4

A Quantum Number-based (n-l-m) Model for Power Grid Analysis

Here by taking a unitary quantum field view on the power grid, we discover a new structural and functional property of complex networks and name it *z-direction radical distance*, built on the principles of quantum system angular motion (the azimuthal motion or l-motion) and Heisenberg uncertainty.

The l-motion-based radical distance is conceived as a fundamental complex network property bijective with energy by nature. With that, we show that radical distance is bijective with energy and observable, thus by associating z-direction axis with fault location, radical distance can quantify the distribution of transient energy influx in macroscopic power grids.

Different from the known complex network properties such as betweenness centrality, radical distance represents a profound non-small-world attribute of complex networks corresponding to complex energy distribution, that penetrates the boundary between the quantum world and macroscopic complex networks, at least from a modeling perspective.

We hope that the defining intrinsic nature of radical distance, combined with striking statistical tendencies exhibited in an estimation of energy distribution on power grid, presents a stimulating thread for exploitation and utilization of hidden quantum effects in natural and man-made complex networks, from an azimuthal (l-motion) perspective. This is unprecedented in the current literature of network science.

4.1 Quantum number-based modeling

Before postulating the quantum number-based model, the basic description of quantum numbers in atom structure model is introduced first.

4.1.1 Fundamental rules of quantum number theory

Quantum numbers are used to specify the properties of orbitals and the properties of electrons in orbitals. In the atom model, the state of electron and the structure of the electrons within an atom are typically described by 4 parameters, and each of them is characterized with a designated quantum number. Quantum numbers define the rules of electron location and orbital filling orders.

Quantum numbers are quantities and tools to completely describe the dynamics and the relation with the energy levels of electrons in an atom model.

In quantum number theory, quantum numbers are actually used to describe the distributions and configurations of electrons in atoms. There is specific relationship between quantum numbers and atomic orbitals, and the fundamental rules are summarized as follows [57]:

- the types of quantum numbers to describe the atom configuration,
- the conventional symbols of quantum numbers,
- the principles for the allowable values of each quantum number,
- the indication of each quantum number and the feature on the basis of the size, shape, direction in space and spin state,
- the description meaning of each type of quantum number in atom configuration, such as shell, sub-shell and orbital,

- the method of how the electrons are distributed among the various atomic orbital, such as the order for the levels and sub-levels, and the numbers of electrons they may contain, and
- the electron configuration principles such as Aufbau scheme, Pauli Exclusion and Hund Rule.

4.1.2 Illustration with atom structure model

In atom model, the quantum numbers are illustrated as follows.

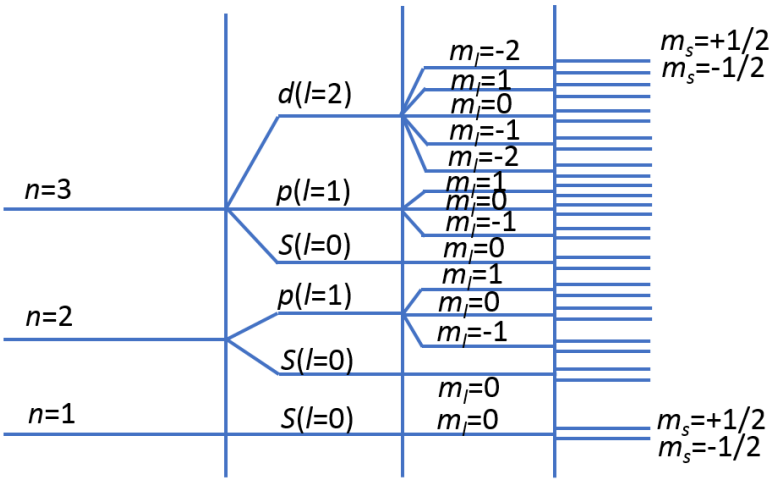

Fig. 4.1: Illustration of 4 quantum numbers describing the states of electron.

Table 4.1: Summary of quantum numbers.

Name	Symbol	Values	Meaning	Indicates
Principal	n	1,2,$\cdots$	shell, energy level	size
Orbital angular momentum	l	0,1,$\cdots$,n-1	sub-shell energy, orbital type	shape
Magnetic	m_l	0,$\pm$1,$\pm$2,$\cdots$,$\pm$ l	orbitals of sub-shell	direction
Spin magnetic	m_s	+1/2,-1/2	spin state	spin direction

Principle quantum number:

- Symbol n: n=1, 2, 3, $\cdots$ (shell)
- Principle quantum number represents the main energy level of the electron and its distance from the nucleus.

- Each orbital has an n value and the larger the value of n, the more energy and the further away from the nucleus it is.
- The total number of orbitals in a energy level is equal to n^2, and the total number of electrons in a energy level is $2n^2$.

Angular momentum quantum number:

- Symbol l: l=0, 1, 2, $\cdots$, $n-1$.
- Orbital angular momentum quantum number describes sub-levels, shapes of the orbital.
- The number of sub-levels in an energy level equals the value of the principle quantum number n, that is, number of possible shapes is equal to energy level.
- Sub-levels are named as s-orbital, p-orbital, d-orbital, f-orbital, $\cdots$
  - s-orbital: l=0
  - p-orbital: l=1
  - d-orbital: l=2
  - f-orbital: l=3
- Shapes of s, p, d, and f orbitals are shown below:

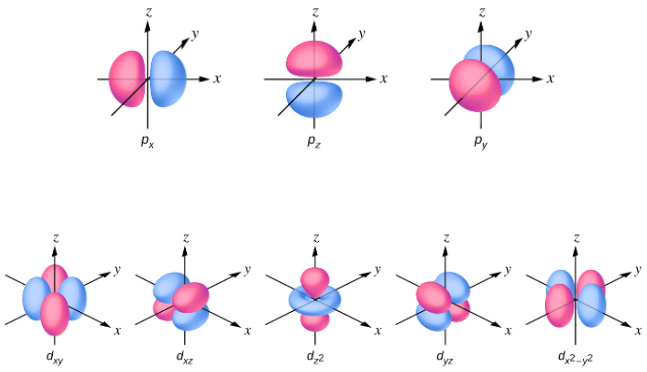

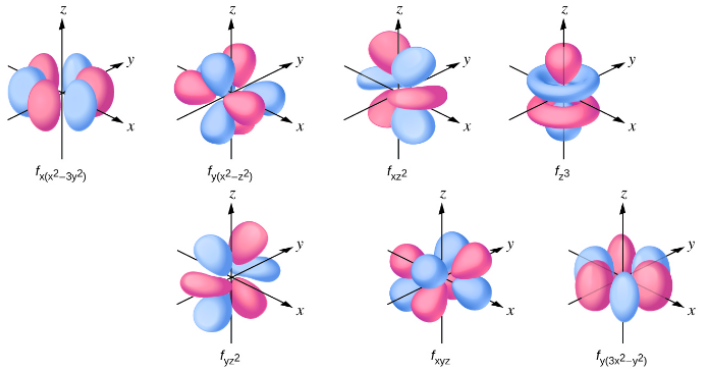

Fig. 4.2: Shapes of the orbitals.

Magnetic quantum number:

- Symbol m_l: m_l=$-l, -l$+1, $\cdots, l-1, l$.
- Determine the orientation of the orbital, how many orbitals there are per energy level and describe a specific orbital among a particular set.

Spin quantum number:

- Symbol m_s: m_s=1/2 or $-1/2$.
- Spin quantum number describes the spin state of the electrons in an orbital and tell whether a electron is spin-up or spin-down.
- There can be two electrons in each orbital and paired electrons must have opposite spins.

4.2 Quantum number-based (n-l-m) model for network

The unitary view permits us to treat the dynamic power grid as a quantum system, then authorizes to use the principles and models of quantum physics to interpret and understand the energy dynamics from a quantum perspective. In this section, a quantum number-based model is proposed.

4.2.1 Model proposition

System description under the hypothetical view:

Under the proposed hypothetical view, the electric power grid with n nodes is considered as an unitary electromagnetic field corresponding a quantum system provided by a cloud of n elementary-unit-like particles i with mass $\mathcal{M}_i$ under a equivalent central potential field $V(r_i)$, in which all particles are entangled so that it can be seen as an one-particle or unitary system evidently, then the coherent state of such a unitary system has n energy eigen-states pertinent to n energy levels.

Energy representation that can be connected to quantum momentum operator:

We consider the energy of this system and complex dynamic interactions using the system Hamiltonian operator. It is known that the system energy state of complex dynamic interactions of a multiple-particles quantum system can be described by central potential Hermitian Hamiltonian operator [58] with the following form,

$$\hat{\mathscr{H}}=-\sum_{i}^{n}\left(\frac{\hbar^2}{2\mathcal{M}_i}\frac{1}{r_i}\frac{\partial^2}{\partial r_i^2}r_i+\frac{1}{2I_i}\hat{\mathscr{L}}^2+\hat{V}(r_i)\right), \tag{4.1}$$

where $\mathcal{M}_i$ and I_i are the mass and moment inertia of each elementary-unit-like particle, respectively, I_i=$\mathcal{M}r_i^2$. r_i is the elementary-unit-like particle distance from the central. $\hat{V}(r_i)$ is the potential operator. $\hat{\mathscr{L}}$ is the angular momentum operator.

With the assumption that there is no position changes of the particles (electric field is unchanged), the r-dependence are factored out, thus the energy change is dominated by rotational energy contributed by a cloud of n particles each with intrinsic angular momentum L_i. Therefore, under the unitary quantum field view, the power system is treated as a quantum system described by the following generic central potential Hermitian Hamiltonian with the origin of reference at its mass centre and negligible

vibrations energy, taking the simple form below,

$$\hat{\mathscr{H}}=\frac{\hat{\mathscr{L}}^2}{2I}, \tag{4.2}$$

where $\hat{\mathscr{L}}^2$ is an angular momentum operator conserved in central potential with the commutation relation, and I is the moment inertia of the system. The energy change is dominated by rotational energy contributed by a cloud of n particles, each with intrinsic angular momentum L_i. The directional net angular momentum are associated with non-commuting spherically rotational symmetric Hermitian quantum operator, $\hat{\mathscr{L}}_i, i=$ $=(x, y, z)$ obeying the Heisenberg uncertainty relation, which has important implication in quantum system [7].

System decolizated state representation:

With a goal of bringing principles and models to bear on complex problems of energy flow on the power grid and seeking a quantum representations on energy flow randomly walking on the graph, the unitary electromagnetic field is considered as an ideal quantum field, that permits entanglement of particles so that they can be considered as a single-particle level, like one with quantum particles that occupy different energy orbitals.

From the quantum perspective, the dynamic behavior of electric power system network can be represented as a quantum state. Consider a electric power system network with n ports, the dynamic behavior of the system can be represented by the state and any state is described as fully as possible by a wave function Ψ, which is a function only of the spatial coordinates of the ports and the time, and determines the port energy and other properties.

Specifically, energy state of the system can be represented by n independent eigen-states

of one-particle in n orbitals with unique energy levels shown below,

$$\begin{bmatrix} \Psi_1 \\ \Psi_2 \\ \vdots \\ \Psi_n \end{bmatrix}_{delocalized} = \underbrace{\begin{bmatrix} C_{11}\, C_{12} \cdots C_{1n} \\ C_{21}\, C_{22} \cdots C_{2n} \\ \vdots \quad \vdots \quad \vdots \quad \vdots \\ C_{n1}\, C_{n2} \cdots C_{nn} \end{bmatrix}}_{\text{related to } J} \begin{bmatrix} \psi_1 \\ \psi_2 \\ \vdots \\ \psi_n \end{bmatrix}. \tag{4.3}$$

Each elementary-unit-like particle state is associated with all the particles in the system with the weight C_{ij}. The system state can be represented with Ψ as Eq. (4.3), in which each column denotes one elementary-unit-like particle state.

The quantum state wave function of some of the elementary-unit-like particles are delocalized across the whole system instead of localizing between some ports. The behavior of any elementary-unit-like particle contributed by the port is not localized between the two linked ports and it extends over the whole system due to the interactions between ports. The state of elementary-unit-like particle is viewed as quantum delocalized. It is a completely delocalized picture of the linking in the electric power system. The delocalized wave functions of elementary-unit-like particle are called system orbitals.

Introducing quantum numbers:

In this quantum number-based model, quantum numbers n, l, m are introduced to describe the characteristics of and energy state based on probability rather than certainty, and can be used to explain observations made on complex interaction particles. The relations are stated as follows.

- Quantum number n represents the the main energy level of the particle in the field and its average distance of the energy state from the center.
- For each energy level n, it limits a maximum angular quantum number l_{max}=$n-1$, which determines the possible values of quantum number m. Therefore, l_{max} also

indicates the distance.

- For each l_{max}, $m{=}{-}l_{max}, {-}l_{max}{+}1, \cdots, 0, \cdots, l_{max}{-}1, l_{max}$, where $m_{max}{=}l_{max}$, and the number of possible values of m is $(2l_{max}{+}1)$.

- Different ms with different values represent different orbitals, where ms with negative values are mirroring orbitals. n particles occupy orbitals with different values of $|m|$. The total number of orbitals with different values of $|m|$ is $m_{max}{+}1{=}n$. The sum of different values of $|m|$ is $l(l{+}1)$. n particles occupy these $l{+}1{=}n$ orbitals. There are two possible states for the particles on these orbital, that, m can be positive and m can be negative (mirror orbitals).

With the quantum number-based (n-l-m) model, energy state of a n-particles quantum system can be represented by n independent eigen-states of one particle in n orbitals with unique energy levels. Orbital angular quantum number l represents an independent angular motion, pertinent to the rotational energy at orbital n, and $l_{max}{=}n{-}1$. Magnetic quantum number m is a set of unique consequent integers determined by l, with the total absolute-value summation equal to $l(l{+}1)$. Since such a motion is parameterized by quantum angular momentum number l, we call l-motion herein after.

The total number of energy state representing orbitals with different values of $|m|$ is $l_{max}{+}1{=}n$. n particles occupy orbitals with different values of $|m|$.

Further explanation of the state of quantum number-based model:

Considering the quantum number-based (n-l-m) model for a quantum system of n entangled particles, the energy states of the system with n particles are characterized by n independent energy eigen-states of one-particle in n orbitals with unique energy levels, which are determined by principle quantum numbers n, angular quantum number l, and magnetic quantum number m. Each energy level is assigned to each particle. n energy levels pertinent to n particles.

4.2.2 Properties of the model

4.2.2.1 One to one relation between $|m|$, particle and energy state

In this subsection, we consider the one-to-one relation between one $|m|$ with certain value, one particle i, one energy state n_i, the number of $|m|$ and n.

The n-l-m model embeds a useful primitive relation of one-to-one correspondence desired. Considering the largest orbital angular quantum number l_{max} for given n in a n-particle quantum system represented by the quantum number-based model, with the knowledge that the magnetic quantum number m has n unique absolute values ($|m|$) ranging from 0 to l_{max} in steps of one, the total number of energy state representing orbitals with different values of $|m|$ is $l_{max}+1=n$. n particles occupy orbitals with different values of $|m|$. Each particle is characterized by a $|m|$ value and an important observation is obtained that there is a one-to-one correspondence between one $|m|$ with one value and one particle associated with one energy state.

Another important observation is that, there are n different values of $|m|$, i.e., the number of $|m|$ equals to n from the quantity, which means that there is a one-to-one correspondence between $|m|$ value to energy level n. It can be concluded that with such a n-l-m uniqueness, a desired one-to-one correspondence between $|m|$ integers and integers of n-orbital energy levels is admitted that is guaranteed by the primitive relation of quantum numbers, so that the usage of one-to-one correspondence between $|m|$ and n entangled energy level of the quantum system is authorized.

To summarized, quantum theory and the property of the model tell us one-to-one relation that each particle is characterized by a $|m|$ value. The value of m and particle are corresponding with each other. One value of $|m|$ only corresponds one particle. Also, there is another one-to-one correspondence between one $|m|$ with one value and one particle associated with one energy state, which relation can be made more precisely with a mapping from a $|m|$ value to a particle and an energy state, i.e, mathematically

can be represented by Eqs. (4.4) and (4.5) as follows inversely,

$$\mathscr{M} : |m| \rightarrow \text{particle } i \cong \text{energy state } n_i, \tag{4.4}$$

$$\text{number of } |m|{=}n. \tag{4.5}$$

4.2.2.2 Uncertainty relationship

Introduce to Heisenberg uncertainty:

It is importantly known that the complex dynamics of the particles for a quantum system behaves in an unpredictable way that follows the Heisenberg uncertainty principles [59]. Here we show that the a specific relation between uncertainty and energy flow of electric power system can be described by the quantum number-based model. In order to find the relation between uncertainty and described energy, we investigate the energy observed at each particle, in the form of surging energy in z-direction.

A quantitative approach to describe the Heisenberg uncertainty relation [7] is as follows. We show an application in explaining the energy uncertainty relationship from the determination relation between uncertainty and observables perspective using quantum number-based model.

Uncertainty relation in terms of defined the imaginary $\hat{\mathscr{L}}_x{-}\hat{\mathscr{L}}_y$ surface and real $\hat{\mathscr{L}}_z$:

For a given reference potential, in the Hamiltonian expression Eq. (4.2), we consider the rotational energy described by angular momentum operators which are conserved in central potentials with respect to the reference, implied by the commutation relation and play a crucial role in our study. A quantitative approach to describe the Heisenberg uncertainty relation [7] is as follows. Hermitian angular momentum operator uncertainty relation can be described in a 3-dimensional $x{-}y{-}z$ Hilbert space. According to the

Heisenberg uncertainty relation [7, 59], angular momentum operator uncertainty relation has the interpretation that for given one randomly chosen polarized direction along the axis z, an ensemble of projective measurements performed on either $\hat{\mathscr{L}}_x$ or $\hat{\mathscr{L}}_y$ will yield a distribution of random outcomes with variances $\Delta\hat{\mathscr{L}}_x$ and $\Delta\hat{\mathscr{L}}_y$. Note that $\hat{\mathscr{L}}_z$ is real with a imaginary circular uncertainty region in an orthogonal plane $x-y$ associated with $\hat{\mathscr{L}}_x$ and $\hat{\mathscr{L}}_y$. The uncertainty of angular momentum in $x-y$ plane determines its constant real z component in the direction perpendicular to $x-y$ plane. Such uncertainty allows available in entangled quantum superposition states, which cannot be derived from classic physics or cycle-based circuit models.

Note that $\hat{\mathscr{L}}_z$ is an operator that yields a number in the z-axis, as the results of circular quantum movement in the imaginary uncertainty surface of $x-y$ characterized by $\hat{\mathscr{L}}_x$ and $\hat{\mathscr{L}}_y$.

Energy uncertainty in terms of the determination relation between uncertainty and scalar constant:

This unitary view permits us to treat the dynamic power grid as a quantum system, then authorizes to use the principles and models of quantum physics to interpret and understand the energy dynamics from a quantum perspective. Under the quantum number-based model, the relation between energy and uncertainty is authorized.

Some researches on application of Heisenberg uncertainty in energy observation suggests that uncertainty variables is fundamentally limited by a scalar Planck's constant [60, 61, 62], i.e., $\Delta E \Delta t \geq$ constant, meaning that it has a constant lower-bound for the product of the uncertainties.

Let's consider the lower boundary of Heisenberg uncertainty principle in the quantum system described by quantum number-based model. Now we apply the constant lower-bound of Heisenberg uncertainty principle to angular momentum operators of the quantum system. We extend the Heisenberg uncertainty relation in term of quantifying the energy occurring at the particles. In particular, let's consider a given reference

potential in the quantum number-based model, and we are interested in the part of rotation energy described in the Hamiltonian expression Eq. (4.2). This energy is the result of quantum circular motion on a finite 3-dimensional $x-y-z$ Hilbert space of rotation-l particles and described in term of Hermitian angular momentum operators which are conserved in central potentials with respect to the reference, implied by the commutation relation. For given one randomly chosen polarized direction along the axis z, in the coherent state, operator $\hat{\mathscr{L}_z}$ yields a lower boundary in the z-axis, as the results of circular quantum motion in the imaginary uncertainty surface of $x-y$ characterized by $\hat{\mathscr{L}_x}$ and $\hat{\mathscr{L}_y}$.

Such uncertainty only available in entangled quantum superposition states, which cannot be derived from classic physics or cycle-based circuit models or not related to any uncertainty of mechanical motion and therefore without any classical analog.

4.2.2.3 Quantification of the quantum uncertainty degree

Considering above Heisenberg uncertainty relation, we define a z-direction after a fault. According quantum mechanical model, projection of the l_{max} on z-direction $l_{max,z}$ is m_z with real number, where m_z=$l_{max,z}$, and m_z indicates a distance. The number of m_z with different values is $2l_{max}$+1. The number of $|m_z|$ with different values is l_{max}+1=n. Maximum projection of l_imax on z-direction is $m_{z,i,max}$, which is a real distance representing the energy state n_i on z-direction in the fully connected unitary electromagnetic field. The value of m_z stands for the projection of distance on z-direction. Quantum numbers l, m are representation of both energy and distance. Note that there is one-to-one correspondence between each value of m_z and each particle. This distance quantized by m_z corresponds to a particle at an energy level related with the average distance from the center. It is also a macroscopic measure of the practical electric power system parameter. We notice distance square is representation of energy.

Introduction of ι:

Let's consider the projection low-boundary of Heisenberg uncertainty on $\hat{\mathscr{L}}_x - \hat{\mathscr{L}}_y$ surface along z-direction of angular momentum $\hat{\mathscr{L}}$ in quantum number-based model. To facilitate the analysis, we further denote $\iota = l_{max}+1$, $(\iota = 1, 2, \cdots, n)$ to associate the maximal angular quantum number of a given energy level (with l_{max}) with respect to a unit reference potential. And one-to-one correspondence of ι to quantum energy states is also authorized by aforementioned n-l-m uniqueness.

Specifically, the denotation of ι is important in that it allows us to find the length between the farmost quantum sub-shelol to the center origin for a given reference potential as $\sqrt{\iota(\iota+1)}$, as schematically depicted in Fig. 4.4. In our model, heterogeneous particle variables with different moment inertia are considered, which can be seen in Fig. 4.3.

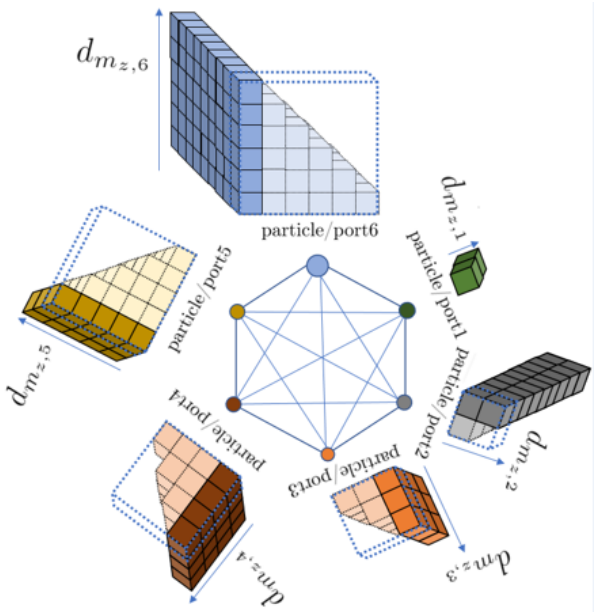

Fig. 4.3: Relative z-direction rotational energy illustration.

Definition of z-direction radical distance:

Aiming at obtaining the needed observability of $\sqrt{\iota(\iota+1)}$ from l-motion, the following framing principle is used. It is known that, by framing the Hermitian operator of a quantum system on angular momentum conserved in a given central potential with the commutation relation (Eq. (4.2)) in a x-y-z system of 3-dimension Hilbert space, the angular momentum in a chosen polarized orientation can be projected to the z-direction

that is real thus observable [7, 60]. Those non-observable uncertainties of angular motion are left on the imaginary $x-y$ surface, characterized by $\hat{\mathscr{L}}_x$ and $\hat{\mathscr{L}}_y$ [61, 63]. Such a framing principle is often used in description of lower-bound of $\Delta\hat{\mathscr{L}}_x\Delta\hat{\mathscr{L}}_y$ associated with Heisenberg uncertainties as an observable projection in z-direction, i.e., a real number in z-direction [7, 60, 61], as proceeded next.

This allows us to define uncertainty based on projection. Here, by adhering quantum quantity $\sqrt{\iota(\iota+1)}$ in above z-direction framing principle, we know that the azimuthal projection of $\sqrt{\iota(\iota+1)}$ in z-direction axis is observable, ready for quantifying the degree of uncertainty of quantum system with respect to the $\hat{\mathscr{L}}_x-\hat{\mathscr{L}}_y$ surface associated with a given l-motion for a given angular quantum number, shown in Fig. 4.4.

This kind of treatment of the projection of quantum number $\sqrt{l(l+1)}$ on z-direction allows us use $|m_z|$ to define a distance in z-direction associated with the energy caused by circular rotational motion in the quantum system. In other words, this distance quantized by m_z corresponds to a particle at an energy level that related with the length from the center. We define an important distance-concept below and call this distance $d_{m_{z,\iota}}$ the z-direction radical distance, illustrated conceptually in Fig. 4.4, which is the projection of $\sqrt{\iota(\iota+1)}$ on z-direction and the distance between the central to particle.

$$d_{|m_{z,i}|} := z-\text{direction radical distance.} \tag{4.6}$$

This indicates the relation between z-direction radical distance and $|m_z|$. The number of $|m_z|$ is also n. The number of z-direction radical distance $d_{|m_z|}$ is n.

Specifically, we use $\sqrt{\iota(\iota+1)}$ to define an important distance-concept associated with the energy represented by uncertain circular motion. The z-radical distance reflects the projection of $l_{imax}(l_{imax}+1)$ on z axis, and the distance between the central to particle, which is illustrated in Fig. 4.4. By letting the angle between z-direction of azimuthal motion or l-motion and the uncertainty $\hat{\mathscr{L}}_x-\hat{\mathscr{L}}_y$ surface by γ_ι, we find the following

important quantity and name it as radical distance, and the expression of measurable z-direction radical distance can be defined as follows,

$$d_{m_{z,\iota}}=\sqrt{\iota(\iota+1)}\cdot\sin\gamma_\iota, \tag{4.7}$$

which is illustrated conceptually in Fig. 4.4. Note that $d_{m_{z,(\iota+1)}}=d_{m_{z,\iota}}+1$, and $d_{m_{z,\iota}}=$ $=|m_z|\approx\iota$ if $\iota_j\gg 1$, where $\iota=1,2,\cdots,n$, n is the number of particles and energy states. By definition, ι corresponds to the energy level and entangled particle.

The radical distance described with Eq. (4.7) represents the most influential positions of particle rotating orbital along z-axis for the given level of uncertainties in $\hat{\mathscr{L}}_x-\hat{\mathscr{L}}_y$ surface. According the quantum number-based model, $d_{z,i}=|m_{z,i}|$ thus has one-to-one relation to energy level n_i.

The energy states of the system with n particles are n independent one-particle energy eigen-states associated with n energy levels, which are determined by principle quantum numbers n, angular quantum number l, and magnetic quantum number m. Each energy level is assigned to each particle. Based on the quantum number-based model, the relation of the distances represented by these quantum numbers is shown in Fig. 4.4.

An important observation is obtained that z-radical distance $d_{|m_z|}$ quantized by $|m_z|$ has an one-to-one relation to each particle, energy level n_i, and the particle total rotational energy $l(l+1)\hbar^2$ in homogeneous unit momentum inertia system that will talk about in the following section.

Fig. 4.3 is the conceptual illustration of surging energies of 6-particles quantum system, quantified by 6 radical distances in observable z-direction in 6 different colors, correspond to the generators located at 6 ports in the power grid. Different ports are represented by different colors with unit blocks. For each port, different unit blocks represent the different moment inertia of the generators. The number of unit blocks showing that radical distance is determined by the absolute values of quantum number

m. The number of unit block with dark color indicates the z-direction radical distance, which can represent z-direction surging energy. The number of unit blocks with light colors indicates the different possible distance coming form the different possible value of quantum number $|m|$. The middle of Fig. 4.3 is the completed graph representation of unitary interconnected electromagnetic fields.

Fig. 4.4 is the conceptual illustration of z-direction radical distance $d_{m_{i,\iota}}$ of quantum system and the relation with entangled particles, which is the observable distance representing azimuthal projections of length $\sqrt{\iota(\iota+1)}$ in observable z-direction, perpendicular to the imaginary $x-y$ surface of quantum uncertainty.

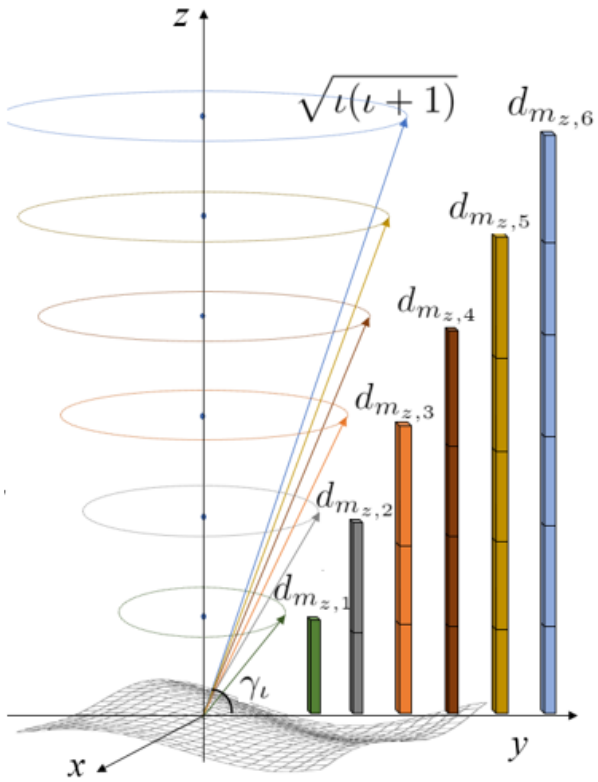

Fig. 4.4: Explanation of distance and particle relation.

Remarks on z-direction radical distance:

Different from the graph distance of classic complex networks theory or electrical distance from electric engineering theory, the z-direction radical distance is a set of sequential integers defined based on the quantum number-based model, serving as one of

the fundamental proprieties of complex network from a quantum perspective.

The radical distance described with Eq. (4.7) represents the most influential positions of particle rotating orbital along z-axis for the given level of uncertainties in $\hat{\mathscr{L}}_x - \hat{\mathscr{L}}_y$ surface. Specifically, the radical distances is a resultant outcome or reflection of the maximum impact of strength or loading conditions of a dynamic complex network at the $\hat{\mathscr{L}}_x - \hat{\mathscr{L}}_y$ surface that has the property of saturating a Heisenberg uncertainty relation.

The concept of distance is very important, which is completely different from classic complex network method. We can get the connection between classic and quantum analysis using distance. Two distances are different. This radical distance is defined from quantum number-based model and it is a fundamental network property from quantum perspective.

This distances is a reflection of the maximum impact of strength or loading conditions of a dynamic complex network from the quantum perspective at the given position from the quantum perspective, which has the property of saturating a Heisenberg uncertainty relation.

4.2.3 Remarks

The remarks of quantum number-based model are as follows.

In order to understand how the system structure may effect the performance of the electric power system, a power network physics model was proposed based on the hypothetical view, extended physics illustration with boundary field and neighboring field, and the experience and knowledge in power grid, which can be used to help us to get better understanding of some characteristics of the electric power system and to solve some existing complex problems potentially.

The integrated quantum number-based model is based on the fundamental physics principles other than the electric circuit rules (KCL and KVL) with linear representation

of connection using impedance, which are different from some similar concepts used in complex system analysis, particularly in electric power system like the link strength, electrical distance and so on [45, 64].

The quantum number-based model of electric power system is a new model based on the assumptions of quantum effect and relativistic effect. This assumption allows that B-F and N-F are joint together. Based on the combined B-F and N-F effect, the unified interconnected electromagnetic field is taken. The quantum number-based model is not supported by existing power system theory and knowledge, which is the non-classic standpoint, and not electric circuit theory based model.

The quantum number-based model allows the electric power characteristics are studied in a wide time scale. Especially, it may provide the potential solution for the transient study of electric power system no matter the frequency.

4.3 Estimation of energy flow in network

The developed quantum number-based model with a unitary electromagnetic quantum field can be applied to study transient energy flow during the initial transient period following a untoward event in electric power grid. The unitary quantum field is gauge and Hermitian symmetric during the transient period, and permits delocalized energy exchanges at the critical ports or nodes of electric power grid, thus authorizes an extension of the basic quantum number-based model and the Heisenberg uncertainty principle to represent energy flow using surging energy in z-direction and exploit a specific energy influx in power grid.

Next we will show that radical distance can be used to quantify the impact of network uncertainties in terms of energy, or the surging energy more precisely.

4.3.1 Relationship between distance and energy

Let's focus on a specific relation between the energy and uncertainty that related to the problem we studied that is the relation between uncertainty and surging energy and energy influx of electric power system dynamics.

Many studies of Heisenberg uncertainty [60, 61, 62] consider that uncertainty variables can be limited by a real constant measurement. In the quantum model, energy can be measured at each particle, in which we can define the direction of energy flow through the particle along as z axis. Similarly, in the physical dynamics electric power system, only energy can be measured at each physical port. In each port, we can define the direction of energy flow through the physical port along as z axis. Mathematically, taking the view of tensor analysis, z axis is determined by a surface, and we define the $\hat{\mathscr{L}}_x - \hat{\mathscr{L}}_y$ surface perpendicular to z axis. From the co-variant and contra-variant principles in tensor analysis [65], the resulting z component of the energy flow at each particle are said to be referred to the imaginary $x-y$ surface (coordinate transformation is needed). z is physical direction of energy, while $x-y$ surface is referred to as one in the unitary field which is imaginary with Heisenberg uncertainty.

Connect from distance to energy:

Let's denote the rotation energy defined in Eq. (4.2) with distance which is the result of rotation of uncertainty movement. Since z-direction radical distances quantified by quantum number is a resultant outcome or reflection of the maximum impact of strength or loading conditions of quantum system at the $\hat{\mathscr{L}}_x - \hat{\mathscr{L}}_y$ surface, according to Eq. (4.2), the energy associated with resulting rotational quantum motion of particle over a uncertain $x-y$ surface associated with $\hat{\mathscr{L}}_x$ and $\hat{\mathscr{L}}_y$ can be considered as a surging energy in z-direction $\epsilon_{z,i}$ perpendicular to $\hat{\mathscr{L}}_x - \hat{\mathscr{L}}_y$ surface, in terms of total rotational energy $l(l+1)\hbar^2$ and the energies surging at individual particles.

The resultant rotational quantum movement of particle over a uncertain $x-y$ surface

associated with $\hat{\mathscr{L}_x}$ and $\hat{\mathscr{L}_x}$ can be considered as a surging energy in z-direction $\epsilon_{z,i}$ perpendicular to $\hat{\mathscr{L}_x}-\hat{\mathscr{L}_y}$ surface.

Specifically, inherent uncertainty in $\hat{\mathscr{L}_x}-\hat{\mathscr{L}_y}$ surface is bounded by a fundamental real precise limit in z-direction. Here we can show that it can found that the maximum of this real-limit number can be used to quantify the energy, including rotational energy (associated with l^2) and the surging energy in z-direction (associated with m_z) at the particle.

4.3.2 Quantification of network energy flow

Now we extend Heisenberg uncertainty projection to quantify the *surging* energy occurred at the particle and angular momentum operators uncertainty relationship from a determination relation between uncertainty and constant energy perspective, using the quantum number-based model.

In order to find the relation between uncertainty and described energy, we investigate the energy observed at each particle (surging energy in z-direction). Next, we show that z-direction radical distance can be used to represent the energy as follows.

Total rotational energy:

For a given reference potential, in the Hamiltonian expression Eq. (4.2), we consider the rotation energy described by angular momentum operators which are conserved in central potentials with respect to the reference, implied by the commutation relation and play a crucial role in our study. A quantitative approach to describe the Heisenberg uncertainty relation [7] is as follows.

According to the intrinsic energy-number relation offered by quantum number-based model, it is known that the relation between quantum number and energy level are bijective, that energy of quantum system can be represented with quantum number. e.g., $m^2\hbar^2$ and $l(l+1)\hbar^2$ with unit moment inertia, are representations of energy expressions

of a quantum system with unit momentum inertia.

In homogeneous unit momentum inertia system, surging energy in z-direction is quantified by $m_z^2\hbar^2$, which is a maximum energy generated on particles very fast, where $m_z{=}{-}l, -l{+}1, \cdots, 0, \cdots, l{-}1, l$, which is the observable energy at port i based on the mapping relation of a set of $|m_z|$ to each particle i.

Similar, we can represent the total rotational energy of l-motion for a given l with respect to z axis with $l(l{+}1)\hbar^2$, surging at particles on quantum orbitals index by non-negative magnetic quantum number or energy level n.

z-direction surging energy:

Since radical distance $d_{m_{z,\iota}}$ is defined as a quantum-number-based projection in z-direction that is observable, it can be used to quantify the fraction $(\sin\gamma_\iota)$ of the maximum rotational energy observed in z-direction with $\hbar^2 d_{m_{z,\iota}}^2$. We call this z-direction rotational energy as surging energy in z-direction, which is a maximum energy generated on particles and can be quantified with radical distance $d_{m_{z,\iota}}^2\hbar^2$. Therefore, let's call $\hbar^2 d_{m_{z,\iota}}^2$ $\underline{z\text{-direction surging energy}}$ because it corresponds to the energy surging at each port of a quantum system, as illustrated in Fig. 4.3.

Generic unit z-direction surging energy:

The primitive relation of quantum number-based model allows us to allocate the surging energy and its distribution using magnetic quantum number. Knowing that magnetic quantum number m is pertinent to a given l_{max} corresponds to n entangled particles, thus, for the different possible values of $|m_z|$ for given l_{max} corresponding to each particle i in quantum number-based model, and the total value of $|m_{z,i}|$ is $\sum_{i=-l}^{l}|m_{z,i}|$, so the total length of radical distance is $2\sum_\iota d_{m_{z,\iota}}$. Thus, for a given l_{max}, a generic unit z-direction surging energy associated with a underlying radical distance can be written

as,

$$\begin{aligned}\epsilon_{z,i}&=\frac{m_{z,i}^2\hbar^2}{\sum_{i=-l}^{l}|m_{z,i}|}\\&=\frac{\hbar^2 d_{m_{z,\iota}}^2}{2\sum_{\iota} d_{m_{z,\iota}}},\end{aligned}\tag{4.8}$$

where $2\sum_{i=-l}^{l} m_{z,i}^{+}=\sum_{i=-l}^{l}|m_{z,i}|$, and $i=1,2,\cdots,n$.

Note that given the total rotation energy $l(l+1)\hbar^2$ the real surging energy can be seen as the energy surging from uncertain rotation energy in $\hat{\mathscr{L}}_x-\hat{\mathscr{L}}_y$ surface at the particle i.

This exploration shows the intrinsic relationship between energy and distance with quantum number-based model.

The ratio of z-direction surging energy with respective to total rotational energy:

According to Heisenberg uncertainty principle, it is easy to tell that the ratio of z-direction surging energy with respective to total rotational energy can be expressed with $\frac{d_{m_{z,\iota}}^2\hbar^2}{2\sum_i d_{m_{z,\iota}}}/l(l+1)\hbar^2$.

The generic surging energy ratio $r(\epsilon_{z,i})$:

In this model, heterogeneous particle variables with different moment inertia are considered, which can seen in Fig. 2.4. For a heterogeneous system with rotational inertia ratio, considering the microscopic rational inertia ratio, the built-in energy-number relation also renders an easy expression of moment inertia $p_i=I_i/\sum_i I_i$, so the general surging energy ratio in z-direction $r(\epsilon_{z,i})$ is obtained as follows consequently,

$$r(\epsilon_{z,i})=\frac{1}{p_{z,i}}\frac{d_{m_{z,\iota}}^2/2\sum d_{m_{z,i}}}{l(l+1)}.\tag{4.9}$$

Eq. (4.9) is the formula can be used as a metric of surging energy at every particle i, and its distribution density function ($\rho(\cdot)$) after being normalized by total energy of l-motion.

4.3.3 Remarks

This exploration shows the intrinsic relationship between energy and distance with quantum number-based model. As energy is truly scaled in both micro and macroscopic world, this energy and distance relation in Eq. (4.9) sheds some lights on using distance to find energy flow property in the electric power grid under the integrated hypothetical view.

1) The energy relations derived in Eqs. (4.9) and (4.11) represent the relation between energy uncertainty and distance from quantum perspective.

2) The Gauge field and observables formalized as Hermitean operators, uncertainty of the hypothetical view allows to use math tools or coordinate change such tensor analysis [66] to connect both quantum models Eqs. (4.9) and (4.11) and real world complex network or power grid models shown in Eq. (3.1) without change the energy nature and characteristics.

Next we will show that despite from its quantum origin, a real world counterpart of this radical distance can be found to quantify the energy influx as the results of disturbance in a network.

4.4 Energy influx estimation in power grid

In this subsection, a specific transient energy in the power grid based on the quantum number-based model is exploited. Specifically, we show that under the integrated hypothetical view, how the Heisenberg uncertainty principle [7] and quantum number-based model can help us exploit the energy transient in power grid.

4.4.1 Energy influx in power grid

Energy flow over the power grid is an inherent network process. The energy transient is the result of a dramatic deviation of the synchronously linked electromagnetic fields from the known or predicted sinusoidal states, to some highly uncertain, possibly chaotic, states of mechanical curve. The resultant complex current spikes induce rapid energy influxes at all interconnected components throughout the power grid. Propagation of energy transient over the electric power grid, particularly during initial period following an untoward incident (often known as the first swing period lasting a few cycles or less), directly affect the grid stability and resiliency.

During the first swing of transient period following an untoward incident, the distribution and magnitude of propagating energy immediately impacts the responses of the primary protective schemes of the power grid, as well as the actions of the secondary stabilization controllers. That guards the bottom-line of power grid stability and resiliency, and form the critical front-line for mitigation or against of the risks of large-scale cascading failures and prevention of fragmentation of networked components.

Due to the level of complexity and uncertainty, the distribution and magnitude of the first swing energy transient are very hard to be described even with high-order non-linear inductance models based on the classic electric circuit theory, with a desired level of accuracy, robustness and generality.

Transitional engineering approaches to understanding of impact of energy transient on grid stability rely on well-defined mathematical models built upon the cycle-based family of sinusoidal waves, including the fundamental frequency (50/60Hz) component, according harmonics and residual noises, as well as the simulated time domain dynamic trajectories such as ones generated by solving nonlinear swing equations describing coupled rotating masses of synchronous generators and dynamic flux models describing electromagnetic energy exchanges.

4.4.2 Definition of energy influx with quantum number-based model

Consider the electromagnet transients in a power grid during the initial transient period immediately following a untoward event such as a fault (normally it is called first swing period for a large system or excitation period for a smaller system) as an energy influx. Transient energy and energy influx during the initial response of the power grid immediately after a fault or disturbance, the exogenous variables (such as those representing controller operating conditions) remain without changes, but the endogenous states (such as the magnetic fluxes) are changed which creates energy influx. And this induced energy plays an critical role in many critical operations such as relays settings, automated under frequency controls for prevention of untoward events.

Transient energy influx referred here is an electromagnetic phenomenon in power grid, that energy observed at buses of power grid during the sub-transient period (in the initial stage of energy transient) following an untoward event. Such a transient energy influx lasts only a few cycles or less, but has a direct and determining impacts on the responses of the protective and stabilization control systems, in defending the power grid from cascading failures or network fragmentation. The transient energy influx in this stage has similar complex nature of core excitation of magnetic system or energization of electric system after being turned on/off, but at a much higher level of complexity due to the number of interconnected components and their interactions, which is one of the most complex nature phenomena and difficult to characterize and quantitatively predict priori.

Transient energy influx in power grid is defined here as the port observation or experience (l-observation) of an inherent transient process of complex network caused by some highly uncertain, possibly chaotic mechanical oscillations and energy waves in the bulk power transmission system that happens at the process outset of the transient (t_{0^+}), following a dramatic deviation of synchronously linked electromagnetic fields from a known or predicted stationary sinusoidal state.

Mathematically, the transient energy influx can be illustrated with a multivariate time domain filtration process characterized by a set of frequency domain models and coherent coupling functions, in terms of a Hamiltonian functions denoted by $\mathbf{H}$ or nearby Hamiltonian system, with the following rather illustrative than rigorous form,

$$\mathcal{F}_{\mathbf{X}}(t)=\{\mathbf{X}(s)|\mathbf{H}: t_{0^+}<s\leq t_s\}, \tag{4.10}$$

where $\mathbf{X}=\{X_1,...,X_K\}\in\mathbb{R}_+^K$ denotes a state vector representing the abundance of energy-exchanging quantities of K interconnected components, during the period from t_{0^+} to t_s, before some dominating transient states are revealed at t_s sub-transient ends. t_s represents the end of the sub-transient period that marks the beginning of the transient period in which some dominating states can be identified. In power system analysis, $\mathbf{X}$ can only be described or estimated by frequency domain models or functions that require at least one 50/60Hz-cycle validation, theoretically.

The transient energy influx of power grid in this stage is a complex mechanical oscillations of sub-synchronous transient dynamics, which has similar complex nature of core excitation of magnetic system or energization of electric system after being turned on/off. It is difficult to characterize and predict priori for complex dynamics, but at a much higher level of complexity due to the number of interconnected components and their interactions.

The complex dynamic nature makes it difficult to predict energy transient accurately and robustly with existing engineering theory and methods. Particularly for the energy influx in the sub-cycle time frame, the state of energy flow is too uncertain and complex to describe by the cycle-based sinusoidal family of frequency domain models. In fact, most surprising or hard-to-explain failures of networked component and open questions are pertinent to the complex dynamics of energy transients or energy influx, such as the ones occurred in cascading events.

4.4.3 Estimation of energy influx in power grid

In this work, distance including the z-direction radical distance and electrical distance is the profound bridge to connect classic complex network theory and quantum view. z-direction radical distance is defined from the quantum perspective and its macroscopic representation is also a macroscopic measure of the practical electric power system parameter.

In this subsection, we will show that despite from its quantum origin, a real world counterpart of this radical distance can be found to quantify the energy influx as the results of disturbance in a network.

In particular to establish the transition between the system described by quantum numbers to electric power system, under the unitary view, we choose the resistance in the complete graph obtained from Kron reduction to represent z-radical distance in Eq. (4.7).

Macroscopic proxy of radical distance, defined by quantum number-based model and principles, for estimation of transient energy influx are warranted by its observability and energy nature. As surging energy is quantified with radical distance, which is real measurable quantity in observable z-direction in quantum theory, we are permitted to interpolate between radical distance ($d_{m_{z,\iota}}$) in quantum world and couplings in macroscopic electromagnetic fields of complete graph representation of real power grid. The insights from aforementioned observations on the nature of couplings of complex network led to the idea of connecting graph distance ($D_{i,f}$) in a complete graph to radical distance. Fortunately, relevant research in mathematics offers rich and profound computational tools, such as the theory and methods of network tensor analysis in [48] and [66]. The macroscopic approximation of radical distance for estimation of transient energy influx in power grid can be obtained from graph distance ($D_{i,f}$) in its complete graph representation with the theory and methods of network tensor analysis in [48] and [66].

Here we postulate the following. Consider a practical real world K-buses electric power grid with N ports of interest ($N \leq K$), by introducing $D_{i,f}$, L and P_i, the ratio of energy influx in electric power grid at port i, $R(\mathcal{E}_{i,f})$, can be directly obtained from equation (4.9), which is the macroscopic surging energy in z-direction,

$$R(\mathcal{E}_{i,f})=\frac{1}{P_i}\frac{D_{i,f}^2/2\sum D_{i,f}}{L(L+1)}, \tag{4.11}$$

where $i=1,2,\cdots,N$. $D_{i,f}$ and L are different macroscopic dominating distance measure, which is the physical world representation of quantum numbers in microscopic, and $D_{i,z}$ is graph distance as a macroscopic approximation of z-direction radical distance in the complete graph representation of a complex network for given reference f. They are corresponding to reference uncertainty, different macroscopic dominating distance measures, and the physical world representations of z-direction radical distance in microscopic. Specifically, they are electrical distances in electric power system associated with the port and the system respectively. P_i is the moment inertia, which will be shown in following practical study.

Knowing that theoretically $l(l+1)$ represent rotational uncertainty motion, the total rotational energy because of the rotational quantum motion of uncertainty is not observable and measurable associated with the $\hat{\mathscr{L}}_x-\hat{\mathscr{L}}_x$ surface, but it can be found $l(l+1)=2\sum|m_i|$ based on the property offered by quantum number-based model.

Note that theoretically $L(L+1)$ is a non-observable quantify energy associated with the $\hat{\mathscr{L}}_x-\hat{\mathscr{L}}_y$ surface but can be estimated with $L(L+1)=2\sum D_{i,f}$ according to the primitive relation of quantum number-based model. The computation of $D_{i,f}$ can be obtained from Kron reduction [48].

If there is a fault in the electric power system, there will be different influx energy on different physical ports corresponding to each energy change on different physical ports.

Fault location is considered as a reference.

The construction of Eq. (4.11) from Eq. (4.9) enables an energy-enabled across-boundary penetration of z-direction radical distance from the quantum world into macroscopic world in two fundamental aspects:

1 Surging energy ratio ($r(\epsilon_{z,i})$) for a given unit reference potential built upon quantum theory as well as surging energy distribution ($\rho_i(\epsilon_{z,i})$) provide practical metrics for estimation of energy influx ratio and its distribution ($\rho_i(\mathcal{E}_{i,f})$) for all nodes of interest i, i.e.,

$$\rho_i(\epsilon_{z,i}) \sim \rho_i(\mathcal{E}_{i,f}). \tag{4.12}$$

2 Total surging energy ($\sum_i \epsilon_{z,i}$) and its distribution $\rho_z(\sum_i \epsilon_{z,i})$ among all reference potentials of interest provides practical metrics for estimation of total energy influx ($\sum_i \mathcal{E}_{i,f}$) and its distribution $\rho_z(\sum_i \mathcal{E}_{i,f})$ to reveal the significance of nodes of complex network for a given reference, i.e.,

$$\rho_z(\sum_i \epsilon_{z,i}) \sim \rho_z(\sum_i \mathcal{E}_{i,f}). \tag{4.13}$$

According the energy connection, L and Di, f can be obtained in the practical system, which are approximation of theoretical l and m, and dominating eigen-states representation associated with the studying problems.

Remarks

In this chapter the concept of z-direction radical distance is postulated under a unitary quantum field view. Radical distance is conceived as a structural and functional property of complex networks that penetrates the boundary between the quantum world and macroscopic real systems, thus allows us to quantify dispersion of sub-transient energy in real system with quantum metrics. The relation between radical distance and dispersion

of sub-transient energy in a complex network with respect to a reference potential is quantified. We hope this work can be an impetus that will stimulate further exploitation of exotic quantum phenomena in natural and man-made complex networks.

CHAPTER 5

Demonstration of Practical Application Using a Real World Case

In this chapter, we will show that starting from its quantum origin, a real world counter-party of this radical distance can be found to quantify the energy influx as the results of disturbance in a network. Independent test studies by a regional Transmission Organization (RTO) in estimation of energy influx using real power grid models are present and assert an industrial-grade accuracy of quantification.

5.1 Electro-mechanical stability for power system operation

Power system electro-mechanical stability is an important issue for power system operation. Power system electro-mechanical stability can be considered from two perspectives. The first one is frequency stability, which is from system wide perspective. The other one is angle stability of generators, which is from component perspective. Electro-mechanical stability is directly affected by kinetic energy and potential energy exchange in the network. And the total energy following a fault plays an important role on the dynamics exchange of kinetic energy and potential energy.

The *total energy* in the power system following a disturbance or fault can be represented with the summation of kinetic energy ($W_{KE}(t)$) and potential energy ($W_{PE}(t)$) at any time t, $W(t)$=$W_{PE}(t)$+$W_{KE}(t)$. In this equation, the representations of $W_{KE}(t)$ and $W_{PE}(t)$ are derived from the classical generator model [14, 67, 68], specifically the first swing dynamics. For example, if the classical generator model is considered shown in

Fig. 2.4, $W_{KE}(t)$ and $W_{PE}(t)$ can be represented as,

$$W_{KE}(t)=\sum_{i=1}^{N_g}\int_0^t \frac{2H_i}{\omega_R}\left(\omega_i\left(\tau\right)-\omega_R\right)\frac{d\left(\omega_i\left(\tau\right)-\omega_R\right)}{d\tau}, \tag{5.1}$$

$$W_{PE}(t)=\sum_{i=1}^{N_g}\int_0^t \left(P_{ei}\left(\tau\right)-P_{mi}\right)\frac{d\delta_i\left(\tau\right)}{d\tau}, \tag{5.2}$$

where subscript i refers to the i^{th} generator; $\delta_i\left(t\right)$ is generator rotor angle at any time t; $\omega_i\left(t\right)$ is generator angular velocity at any time t; ω_R is the rated angular velocity; H_i is the generator inertia constant; P_{mi} is mechanical input power of generator; $P_{ei}\left(t\right)$ is electrical output power of generator; and N_g is the total number of generators in the system.

The *total transient energy* refers to the total amount of energy that is accumulated during the fault period through the interaction between kinetic energy W_{KE} and potential energy W_{PE} in the power system. The total transient energy can be represented with the summation of the total kinetic energy and total potential energy at the instant of fault clearing. When the total amount of energy at the instant time t_c of fault clearing is selected as energy reference, the total transient energy [69, 70], T_F, can be expressed based on Eqs. (5.1) and (5.2) as follows,

$$T_F=W_{KE}(t_c)+W_{PE}(t_c)=\frac{1}{2}\sum_{i=1}^{N_g}\frac{2H_i}{\omega_R}\left(\omega_i\left(t_c\right)-\omega_R\right)^2. \tag{5.3}$$

In Eq. (5.3), variables ω_R, H_i, and N_g are known for a given system. Thus, the total transient energy T_F varies with generator angular velocity $\omega_i\left(t_c\right)$. That is, determining the total transient energy needs to evaluate generator angular velocity, which is one of variables characterizing the dynamics of a power systems. The dynamics are described by a set of DAEs. Thus, determining generator angular velocity needs to solve the

DAEs. Note that when the advanced modeling of generators and controls are used in a power system, the set of DAEs becomes very complicated. Traditionally, the set of DAEs are solved by time domain simulations.

In the experiment with real world model, everything is from time domain simulation and the actual operational models.

Thus, the following procedure can be used to evaluate the total transient energy in Eq. (5.3) for a power system following a given fault: 1) Prepare parameters required to run a simulation for determining the dynamics of the power system. 2) Apply the given fault in the power system. 3) Solve the set of DAEs by time domain simulations to determine angular velocity of all generators in the system at given fault clearing time t_c. 4) Evaluate the total transient energy in (5.3) using the angular velocity of all generators and other parameters such as ω_R and H_i known for the power system.

5.2 Descriptions of demonstrative experiment

Now we present a usage of radical distance in estimation of transient energy influx with real world power flow and dynamic system models of the power grid manged by ISO-New England in the North American Eastern Interconnection (with 4236 buses, 4773 lines, and 230 generators). The US and ISO-New England power grids are shown in Fig. (5.1).

The experiment follows the standard procedure of dynamic stability analysis: a 3-phase short-circuit fault is first introduced at a bus b_z to create energy transient and then the distribution of transient energy influx at all generators of interest is evaluated in the power system. This procedure is repeated for various 177 fault locations (only 345kV buses are included due to space limit). Two methods will be used: radical distance-based structural analysis using Eqs. (4.7), (4.8), (4.9) and (4.11) and model-based time domain simulations.

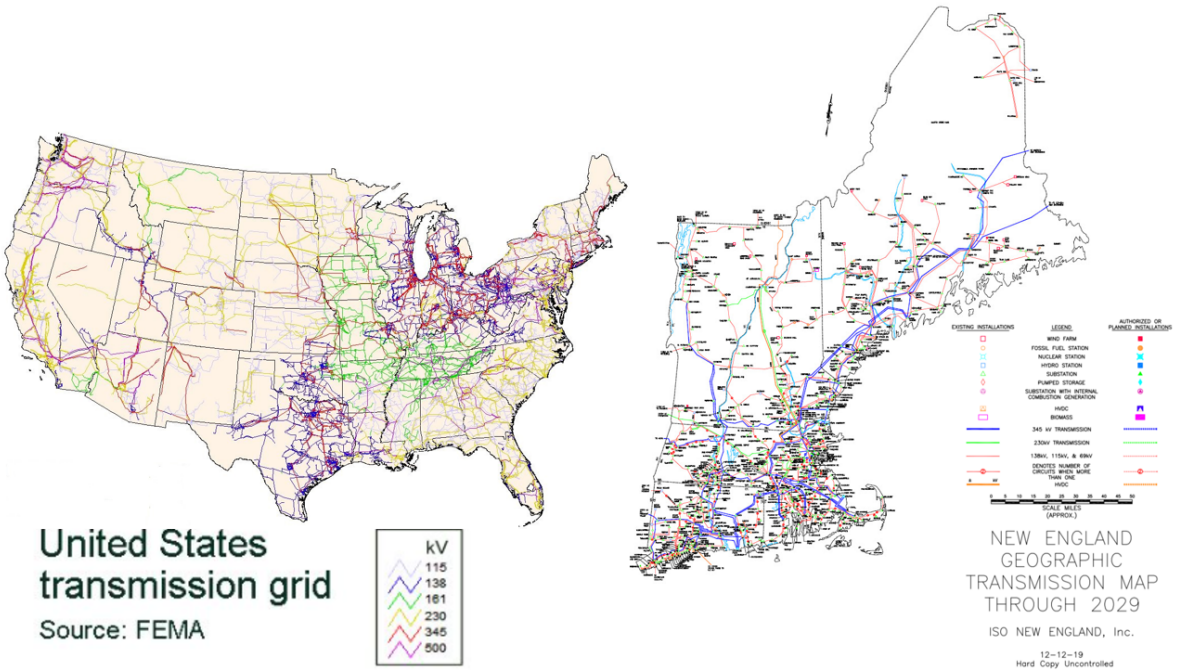

Fig. 5.1: US and ISO-New England power grids.

In the structural analysis, fault bus b_z is considered as the reference for z-direction. $D_{i,z}$ in Eq. (4.11) is determined by the graph distance between generator bus i and fault bus z which can be found in $(N+1)$-reduced matrix from the Laplacian ($\mathbf{L}$) matrix of power grid using the methods of network tensor analysis [66, 71], i.e., $D_{i,z} := B^{\dagger}_{ii} + B^{\dagger}_{zz} - 2B^{\dagger}_{iz}$, $i, z \in (1, 2, \cdots, N)$, where $\dagger$ represents the Moore-Penrose pseudo inverse [71, 72, 73]. P_i in Eq. (4.11) is obtained from the dynamic system model. These are all information needed for radical distance-based structural analysis, no time domain modeling and simulation needed.

Time domain dynamic simulation and validation are done independently by the research group in ISO-New England using commercial Transient Security Assessment Tool (TSAT). The fraction of energy influx at each generator port i is measured based on the change in kinetic energy of each generator $\Delta W_{KE,i}$ during the sub-transient period of 5 cycles with $\sum_i^N (\omega_i - \omega_0)^2 P_i/\omega_0$, where ω_0 is the generator rated velocity; ω_i is the angular velocity of generator i, which is the result obtained from time domain simulations with TSAT.

Having described the set-up of the experiment, we proceed to report its results. The comparative studies and results generated by z-direction radical distance-based structure analysis and time domain simulations are shown using the the real power grid described above.

5.3 Results of experiment

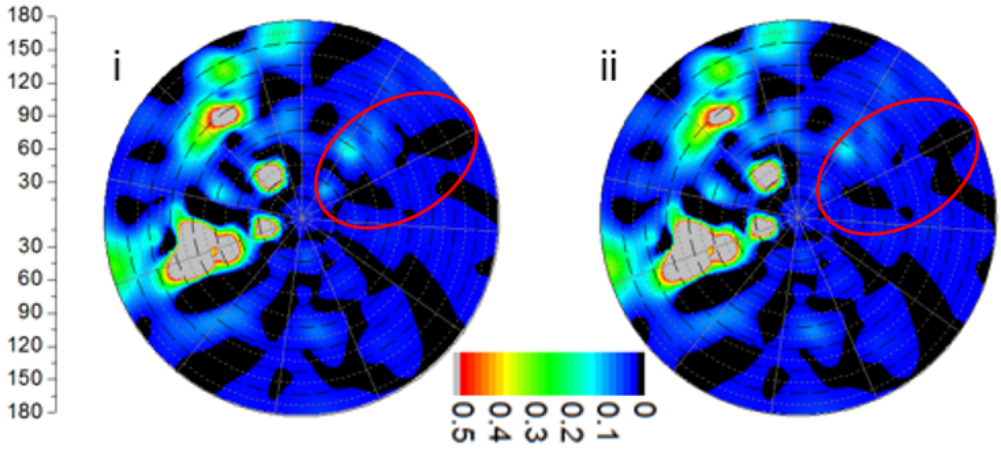

Fig. 5.2: Polar contour maps of energy influx.

Experiment results comparisons of time domain simulation and z-direction radical distance-based structure analysis are described in Figs. 5.2, 5.3 and 5.4, where, Fig. 5.2 is the polar contour maps of energy influx obtained from distance-based structural analysis (`i`) and time domain simulation (`ii`), respectively, in which the energy levels are colored in a range between 0 (black) to 0.5 (red) to show the distributions and boundaries of energy influx. (Two additional levels are added to represent values less than or equal to 0 and greater than 0.5 using black and gray label, respectively.) Angular coordinates represents the 230 generators and radius represents 177 fault bus locations. Fig. 5.3 is the statistical consistency is confirmed with scatter patterns, distribution histograms, and a high correlation coefficient. Fig. 5.4 is the plot of fault severity levels at different locations in decreasing order and the energy of maximum error in two regions (I) and (II). Ultra low errors in region I assert that there is no significant discrepancy in results

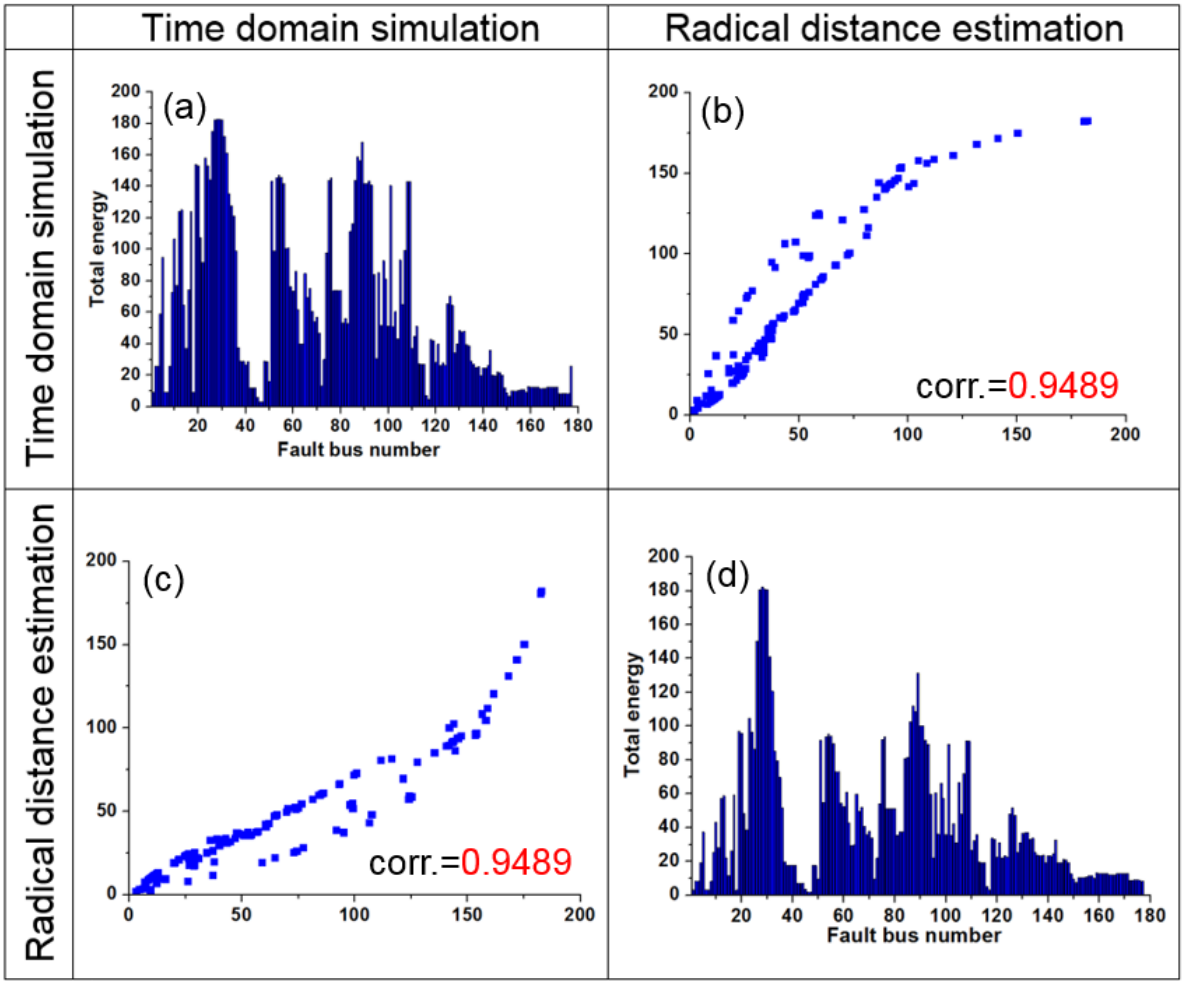

Fig. 5.3: The statistical consistency.

from two methods till the level of severity of faults becomes very low: energy of the maximum error is less than 2.72% for 78 locations of serious fault with the total energy influx over 29.62%. Region II starts from a maximum error of 11.30%. Although the overall maximum error is up to 95.41% (with a fault severity level of 14.38%), the errors in region II are not considered due to the lower severity of fault in practice.

Fig. 5.2 shows the comparison of transient energy influx distributions obtained from the z-direction radical distance-based structural analysis as described in Eq. (4.11-4.12) and time domain dynamic simulation in polar contour map (Fig. 5.2.-i and Fig. 5.2.-ii). Angular coordinates of contour corresponds to the locations of a fleet of 230 generators managed by ISO-New England, while radius corresponds the 177 fault locations. Fig.

5.2.-i and Fig. 5.2.-ii exhibit a remarkable similarity of contour patterns such as pattern intensity, mutual gradient, etc.

The fault energy estimated by distance-based structure analysis is compared with the one evaluated by time domain simulations in the system. Fig. 5.3 shows the result consistency from a statistical perspective in terms of distribution of total energy influx as described in Eq. (4.13) for all fault locations (345kV buses from bus 1 to bus 177) in ISO-New England. It can be seen from Fig. 5.3 that at each fault location, the magnitudes of fault energy estimated by distance-based structure analysis is high correlated with the one evaluated by time domain simulations. A correlation coefficient of 0.9489 confirms the high-degree of consistency in terms of statistical measures such as histogram, scatter distribution, etc.

For practical power system analysis and potential practical applications of the strong dependence of the total transient energy on grid structure, a high level of consistency in statistical measure showing in Fig. 5.2 and Fig. 5.3 may not be adequate for making important engineering decisions, particularly for operational decisions to maintain extra-high reliability of power grid. We further quantitatively analyze the discrepancy resulting from the structural representation of the total transient energy for each individual fault location. The industrial-grade accuracy with non-statically comparison of the total transient energy predicted using distance-based structure analysis with the one evaluated using time domain simulations and the examination of the energy of maximum errors are demonstrated in Fig. 5.4.

Fig. 5.4 demonstrates an remarkable accuracy of the radical distance-based structural analysis in terms of degree of discrepancy between two methods. The orange dots represent the levels of total transient energy influx ($\sum_i \mathcal{E}_{i,f}$) (%) induced by different fault locations in a decreasing order of severity and the blue bars represent the levels of energy (%) of the maximum error for given fault locations. In this case study, the error becomes significant when the level of total transient fault energy influx is small

(<29.62%). For a high level of total fault energy influx, meaning a higher severity level (from the maximum (100%) observed to 29.62%), the errors are very small (<2.72%), which is qualified for industrial applications included those in real operation. In practical operations, faults with severity level less than 30-40% are considered as the low severity faults, which are not critical to system reliability. The ultra-low errors in identifying high severity faults show a very good and an industry-grade accuracy for real world applications.

It can be observed that the energy of maximum error is no more than 2.7% for more than 70.4% total energy covering 78 more serious fault bus location. Within the 29.6% total fault energy, maximum of energy error happens at fault bus location with 14.4% total fault energy. It can be concluded that the energy of maximum error is very low when the total fault energy is more than 70.4%.

Remarks:

In this chapter, an applicability of radical distance in real systems is demonstrated with a quantitative analysis of complex sub-transient problem in a real power grid, exhibiting striking statistical tendencies with an industrial-grade accuracy, which seems unprecedented in the current literature of complex networks. We hoped this work can be an impetus that will stimulate further exploitation of exotic quantum phenomena in natural and man-made complex networks.

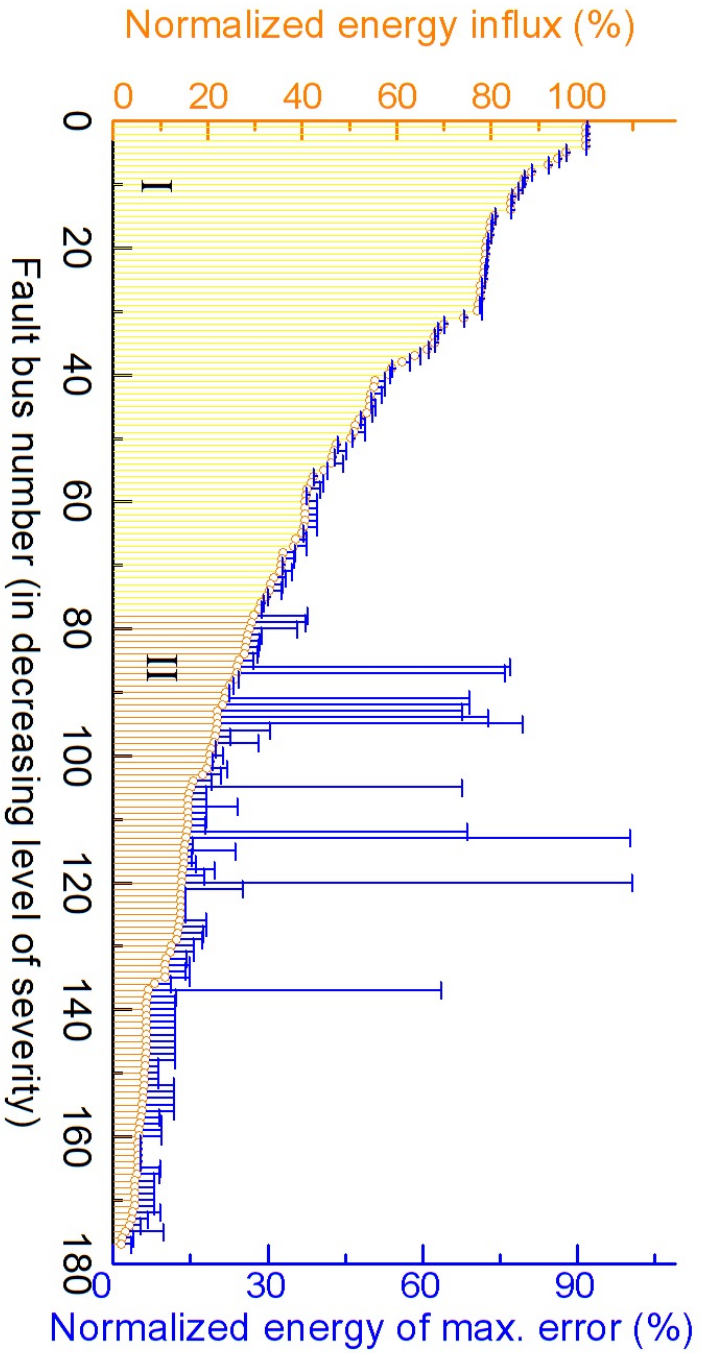

Fig. 5.4: Plot of fault severity levels at different locations in decreasing order and the energy of maximum error in two regions I and II.

CHAPTER 6

Conclusions and Future Works

6.1 Conclusions

The efforts to develop a ubiquitous view of complex networks to understand, predict, or govern system behavior have created both excitement and skepticism about to what extent the knowledge of network structure can be used.

The work is motivated from recent works on unification of power system models with port-Hamiltonian system [38, 43, 47] and applications of complex networks methods in power grid analysis [21, 24, 48, 51].

Particularly inspired by 1) an universal interpretation of electrical distances in power grid and graph distances of complex networks as various manifestations of electromagnetic linkage [47], and 2) mathematical reformation of a fundamental power flow model into a picture of "simultaneous random walk on complete graph" representation [51], we exploit transient energy influx in power grid as a complex-network phenomenon from a quantum perspective: we first regard the power grid with n ports of synchronized components as a unitary gauge electromagnetic field with quantum coherence that is gauge and Hermitian symmetric quantum system, that is represented by a complete graph, to obtain the permissions of 1) investigating the power grid with localized ports as a delocalized quantum system, and 2) using quantum theory and methods.

Further, this dissertation reports a new structural and functional property of complex networks from a quantum perspective, which we call radical distance. Specifically, with the quantum number-based model, we reference and name an important z-direction radical distance, which is the projection of a quantum-number-based length associated with l-motion in the observable z-direction of 3-dimension Hilbert space, with z for the

observable direction as a unit reference orbital potential, and $x-y$ for the uncertainty surface as the results of l-motion.

Restricted by the principles of quantum numbers and Heisenberg uncertainty, radical distance of each entangled particle corresponds to an on-site surging energy associated with the underlying azimuthal or l-motion in observable z-direction, which authorizes quantum effects to be measurable at macroscopic scale.

With the mathematical tools of network tensor analysis [66, 71], we found that observable radical distance built on quantum theory can describe the transient energy influx in real world power grid.

The defining nature of radical distance and its intrinsic bijectivity with energy, combined with the striking statistical tendencies exhibited in the estimation of energy distribution on power grids, present a stimulating thread for exploration of hidden quantum effects in natural and man-made complex networks.

The discovery of quantum-based radical distance, as a new property of complex networks, may stimulate research interests from various disciplines: 1) striking statistical tendencies generated, seemly unprecedented in current literature of complex networks, helps relieving the growing skepticism about applicability of complex networks theory to real problems, 2) industry-grade accuracy exhibited asserts a promising approach to some complex issues notoriously known in physics and engineering, and 3) clear physics and mathematical foundation offers a new perspective on the emerging field of network science, for searching the key that opens the gate between the quantum world and the macroscopic complex reality.

At last, an independent test study in estimation of energy influx with real power grid is presented, which asserts an industrial-grade accuracy of quantification.

6.2 Publications

This research has resulted in the following publications.

[1] Ji, G., Perera, S., Huang Y., Zhang, Y., Ekic, A., Wu, D. A Comparative Study of Sub-cycle Transient Characteristics of IBR Operating State Switchings. IEEE PES Transactions on Power Delivery. (*under review*)

[2] Ji, G, Perera, S, Huang Y, Wu D. A FDTD-based Simulation Study on Distinguishing Characteristics of Inverter Switching and Pulse Fault During Sub-cycle Transient Period. 8th Eur. Conf. Ren. Energy Sys. 24-25 August 2020, Istanbul, Turkey.

[3] Ji G, Sharma D, Fei W, Wu D, Jiang JN. A Graph-theoretic Method for Identification of Electric Power Distribution System Topology. In2019 1st Global Power, Energy and Communication Conference (GPECOM) 2019 Jun 12 (pp. 403-407). IEEE.

[4] Sharma D, Ji G, Fei W, Wu D, Moses P, Jiang JN. Electric circuit foundation of structural analysis for power systems from a network perspective. Mediterranean Conference on Power Generation, Transmission, Distribution and Energy Conversion (MEDPOWER 2018), 2018 page (5 pp.)

[5] D. Sharma, G. Ji, W. Fei, D. Wu, P. Moses, and J. N. Jiang. Electric Circuit Foundation of Structural Analysis for Power Systems from a Network Perspective. In 11th Int. Conf. on Power Generation, Transmission, Distribution and Energy Conversion, Dubrovnik, Croatia, Nov. 2018.

[6] Fei W, Ji G, Sharma D, Jiang JN. A new traveling wave representation for propagation of energy transients in power lines from a quantum perspective. In2018 North American Power Symposium (NAPS) 2018 Sep 9 (pp. 1-6). IEEE.

[7] Ekic A, Strombeck B, Ji G, Wu D. Assessing Grid Strength Using Effective Site-Dependent Short Circuit Ratio. IEEE Transactions on Power Delivery. (*Processing*)

[8] Wu D, Sharma D, Ji G, Perumalla V, Luo X, Jiang JN. Structural Analysis Based Method for Estimating Critical Clearing Time without Time Domain Simulation. In 2019 IEEE Power & Energy Society General Meeting (PESGM) 2019 Aug 4 (pp. 1-5). IEEE.

[9] Perumalla, V, Gopakumar, G, Javadi, M, Ekic A, Wu D, Ramakumar, R, Ji G, Jiang, J. Limitation of Fundamental Analytics for Fault Transients on Planning of Transmission Systems with High Penetration of Solar PV Resources. 8th Eur. Conf. Ren. Energy Sys. 09-11 June 2020, Istanbul, Turkey.

[10] Ji, G, Fei W, Sharma D, Jiang J. Generalized Graph Energy of Electric Power Distribution Grid and Its Impact on Identification of Physical Grid Topology. 8th Eur. Conf. Ren. Energy Sys. 09-11 June 2020, Istanbul, Turkey.

[11] Almir Ekic, Bennett Strombeck, Di Wu, Guomin, Ji. Assessment of Grid Strength Considering Interactions between Inverter-based Resources and Shunt Capacitors. 2020 IEEE PES GM. Best Conference Papers on Distributed Energy Resources, Inverter-based Devices, and Microgrids.

[12] Milad Javadi, Di Wu, Gangan Li, Guomin Ji, John N. Jiang. Estimation of Transmission System Power Transfer Capability at Competitive Renewable Energy Zones. 2020 IEEE PES GM. 2020 PES T&D Conference & Exposition.

6.3 Future works

Opened up by this dissertation, the following works may be explored for the future research.

- Based on the understanding of the proposed quantum number-based model for network, I believe there are many potential applications. In the near future, First, I will focus on the interface development with real time issue. Specifically, the network structure will be measured with the real time estimation model instead of using the planning model. Based on the real time estimation, the interface will be developed.

- Second, I am planning to do some real time dynamic analysis using measured data. Specifically, I will focus on real time estimation based on the dynamic data measurement instead of using the static data based on the model because the system structure obtained from the measure based estimation is different from the one obtained from the static model.

- Some potential applications would be further explored in the area of power grid dynamics and electromagnetic stability analysis based on the understanding of physics-based analytical framework.

List of Abbreviations

NERC	North American Electric Reliability Corporation
DAEs	Differential and algebraic equations
DC	Direct current
AC	Alternating current
FACTS	Flexible AC transmission system
AVR	Automatic voltage regulator
CCT	Critical clearing time
PEBS	Potential energy boundary surface
TEA	Transient energy automaton
LHS	Left-hand-side
RHS	Right-hand-side
B-F	Boundary-field
N-F	Neighboring-field
RTO	Regional transmission organization
TSAT	Transient Security Assessment Tool

List of Key Symbols

x	vector of state variables;
y	Vector of network variables;
λ	vector of parameters;
n_g	The number of synchronous generators;
$\dot{\delta}_i$	Angle of the i^{th} machine;
ω_i	Angular velocity of the i^{th} machine
M_i	Inertial constant of the i^{th} machine;
P_{mi}	Mechanical power of the i^{th} machine;
P_{ei}	Eectrical power of the i^{th} machine;
ω_R	The reference angular frequency of the system;
E_i	Magnitudes of the voltages of electric machine at internal nodes i;
δ_i	angles of electric machines at node i and i;
Y_{ij}	Magnitude of the admittance between internal node i and j;
Θ_{ij}	Angle of the admittance between internal node i and j;
G_{ii}	Total conductance at internal node i;
δ_i	Rotor angle of generator i;
ω_i	Rotor speed of generator i;
$\Delta\omega$	Change of rotor speed;
$\Delta\delta$	Change of rotor angle;
e'_{qi}	Transient voltages along q axis respectively of generator i;
e'_{di}	Transient voltages along d axis respectively of generator i;
i_{di}	Stator currents of q axis of generator i;
i_{qi}	Stator currents of d axis of generator i;
H_i	Inertia of generator i;

D_i	Damping constants of generator i;
T'_{d0i}	Open circuit time constants for d axis of generator i;
T_{q0i}	Open circuit time constants for q axis of generator i;
X_{di}	Synchronous reactance for d axis of generator i;
X_{qi}	Synchronous reactance for q axis of generator i;;
X'_{di}	transient reactance for d axis of generator i;
X'_{qi}	transient reactance for d axis of generator i;
ω_s	the Synchronized frequency of the system;
V_{ref}	Reference voltage of the AVR;
V_r	Outputs of the AVR;
R_f	Exciter soft feedback;
E_{fd}	Voltage applied to generator field winding;
T_a	AVR time constants;
T_e	Exciter time constants;;
T_f	Feedback time constants;;
K_a	Gains of AVR;
K_e	Gains of exciter;
K_f	Gains of feedback;
Vr, min	Lower limits of V_r;
Vr, max	Upper limits of V_r;
P_{gs}	Designated real power generation;
P_m	Mechanical power of the prime mover;
μ	Steam valve or water gate opening;
μ_{min}	lower limit of μ;
μ_{max}	upper limit of μ;
R	Governor regulation constant;
ω_{ref}	Governor reference speed;
T_{ch}	Time constant related to the prime mover;

T_g	Time constant related to the speed governor;
$V(x)$	Lyapunov or energy function;
V_{cr}	Critical energy;
$V_{KE}(\tilde{\omega})+V_{PE}(\theta)$	Sum of the kinetic and potential energies of the post-fault system;
G	Graph;
$\mathscr{V}$	Set of graph vertices;
$\mathscr{E}$	Set of graph edges;
$\mathbf{M}=(M_{kh})$	Incidence matrix;
$\mathbf{A}=(A_{ij})$	Adjacency matrix;
$\mathbf{L}=(L_{ij})$	Laplacian matrix;
$\mathbf{D}=(D_{ij})$	Degree matrix ;
$T=(t_{kh})$	Sign matrix;
$\Theta_i-\Theta_j$	Difference of phase angles between two buses i and j;
$\mathbf{B}$	Susceptance matrix;
b_i	Susceptance of node i;
b_{ij}	Susceptance of transmission line connecting node i and node j;
B_{ij}	The element in susceptance matrix;
E_f	Fault-induced change of system potential;
$W_{PE,i}^{max}$	Component linking strength;
E_f	Inrush exchange of induced fault energy;
K	Number of buses of power system;
N	Number of ports of power system;
$H(q,p)$	Hamiltonian of the system;
$q=(q_1,\cdots,q_k)^T$	Generalized configuration coordinates for the dynamic system with k degrees of freedom;
$p=(p_1,\cdots,p_k)^T$	The vector of generalized momentum;
$B(q)f$	Generalized forces;
$f\in\mathbb{R}^m$	Input;

C_i	Capacitance of the i^{th} capacitor;
L_j	Inductance of the j^{th} inductor;
$q(t) \in \mathbb{R}^{n_C}$	Vector of capacitor charges at time t;
$\varphi(t) \in \mathbb{R}^{n_L}$	Vector of inductor fluxes at time t;
$\mathbf{J}$	Skew symmetric $n \times n$ matrix;
$H(x_1, x_2)$	Sum of two individual Hamiltonian functions $H_1(x_1)+H_2(x_2)$;
$(L_W)_{N\times N}$	Weighted Laplacian matrix considering the line impedance;
$(L_\Psi)_{N\times N}$	Weighted Laplacian matrix considering the injection power on each nodes;
$(L_{W\Psi})_{N\times N}$	Weighted Laplacian matrix considering the line impedance and injection power on each nodes;
$\mathbf{Z}$	Diagonal matrix of the line impedances;
E	Energy of the particle;
$\vec{p}$	Momentum of the particle;
m_p	Particle mass;
v	Traveling velocity;
h	Planck's constant;
$\hbar$	Reduced Planck's constant;
$\vec{k}$	Wave vector;
λ_w	de Broglie wave length of the particle;
ω	Angular frequency of the particle;
ν	Vibration frequency of the particle;
B-F	Boundary field;
N-F	Neighboring field;
$H_{complete}^{classic}$	Classic interconnected electromagnetic field matrix;
$\hat{H}_{complete}^{quantum}$	Hamiltonian operator of interconnected electromagnetic field;
$\hat{H}_k$	B-F operator;
$\hat{H}_{ij}$	N-F operator;

n	Principle quantum number;
l	Orbital angular momentum quantum number;
m_l	Magnetic quantum number;
m_s	Spin magnetic quantum number;
$\mathcal{M}_i$	Mass of elementary-unit-like particle;
$V(r_i)$	Equivalent central potential field;
I_i	Moment inertia of each elementary-unit-like particle;
r_i	Elementary-unit-like particle distance from the central;
$\hat{V}(r_i)$	Potential operator;
$\hat{\mathscr{L}}$	Angular momentum operator;
L_i	Intrinsic angular momentum;
I	Moment inertia of the system;
$\hat{\mathscr{L}}_i$	Rotational symmetric Hermitian quantum operator;
Ψ	Wave function;
C_{ij}	Weight;
l_{max}	Maximum angular quantum number;
$\hat{\mathscr{L}}_x$	Angular momentum operator in the x-axis;
$\hat{\mathscr{L}}_y$	Angular momentum operator in the y-axis;
$\hat{\mathscr{L}}_x$–$\hat{\mathscr{L}}_y$	Imaginary surface;
$\hat{\mathscr{L}}_z$	Angular momentum operator in the z-axis;
$l_{max,z}$	Projection of the l_{max} on z-direction;
m_z	Projection value of the l_{max} on z-direction;
$m_{z,i,max}$	Maximum projection of $l_i max$ on z-direction;
ι	Maximum angular quantum number plus 1, i.e.,l_{max}+1;
$d_{m_{z,\iota}}$ $d_{m_{i,\iota}}$	z-direction radical distance;
γ_ι	Angle between z-direction of azimuthal motion or l-motion and the uncertainty $\hat{\mathscr{L}}_x$–$\hat{\mathscr{L}}_y$ surface;
$d^2_{m_{z,\iota}}\hbar^2$	z-direction surging energy;

$l(l+1)\hbar^2$	Total rotational energy;
$\epsilon_{z,i}$	Generic unit z-direction surging energy;
$r(\epsilon_{z,i})$	The generic surging energy ratio;
p_i	Moment inertia of the particle;
t_{0^+}	The process outset of the transient;
$\mathbf{H}$	Hamiltonian functions;
$\mathbf{X}$	State vector representing the abundance of energy-exchanging quantities of K interconnected components;
t_s	Sub-transient ends;
$D_{i,z}$	Graph distance;
$R(\mathcal{E}_{\mathrm{i,ref}})$	Macroscopic surging energy in z-direction;
P_i	Moment inertia;
L	Macroscopic dominating distance measure;
$\rho_i\left(\epsilon_{z,i}\right)$	Surging energy distribution;
$\rho_i(\mathcal{E}_{\mathrm{i,ref}})$	Energy influx distribution;
$\sum_i \epsilon_{z,i}$	Total surging energy;
$\rho_z(\sum_i \epsilon_{z,i})$	Total surging energy distribution;
$\sum_i \mathcal{E}_{\mathrm{i,ref}}$	Total energy influx;
$\rho_z(\sum_i \mathcal{E}_{\mathrm{i,ref}})$	Total energy influx distribution;
$W_{KE}(t)$	Kinetic energy;
$W_{PE}(t)$	Potential energy;
t	Time;
$W(t)$	Total energy;
$\delta_i\left(t\right)$	Generator rotor angle at any time t;
$\omega_i\left(t\right)$	Generator angular velocity at any time t;
N_g	The total number of generators;
T_F	Total transient energy;
t_c	The instant time of fault clearing;

$\omega_i(t_c)$	Generator angular velocity at t_c;
b_z	Fault bus;
$\dagger$	Moore-Penrose pseudo inverse;
$\Delta W_{KE,i}$	The change in kinetic energy of each generator;
ω_0	Generator rated velocity;
$W_{PE,i}^{max}$	Component linking strength;
E_f	Fault energy;

Bibliography

[1] NERC, "Available transfer capability definition and determination," *North America Electric Reliability Council*, Jun 1996.

[2] F. Xue, "Transient stability limits of interface flow," in *IFAC Symp. on Power Systems Modelling and Control Applications, Brussels*, 1988.

[3] P. Kundur *et al.*, "Definition and classification of power system stability. IEEE/CIGRE joint task force on stability terms and definitions," *IEEE Trans. Power Syst.*, vol. 19, no. 2, pp. 1387–1401, May 2004.

[4] ISO NE TTC tables. [Online]. Available: http://www.iso-ne.com/trans/ops/limits/ttc/new_england_ttc_tables.htm

[5] P. W. Sauer and M. A. Pai, *Power system dynamics and stability.* Prentice hall Upper Saddle River, NJ, 1998, vol. 101.

[6] B. Stott, "Power system dynamic response calculations," *Proceedings of the IEEE*, vol. 67, no. 2, pp. 219–241, 1979.

[7] J. Geremia, J. K. Stockton, and H. Mabuchi, "Real-time quantum feedback control of atomic spin-squeezing," *Science*, vol. 304, no. 5668, pp. 270–273, 2004.

[8] A. Pizano-Martinez, C. Fuerte-Esquivel, and D. Ruiz-Vega, "Global transient stability-constrained optimal power flow using an OMIB reference trajectory," *Elect. Journal*, vol. 25, no. 1, pp. 392–403, Feb 2010.

[9] D. Gan, R. Thomas, and R. Zimmerman, "Stability-constrained optimal power flow," *IEEE Trans. Power Syst.*, vol. 15, no. 2, pp. 535–540, 2000.

[10] A. Bettiol *et al.*, "Transient stability-constrained optimal power flow," in *IEEE Budapest Powertech.*, Sept 1999.

[11] V. Vittal, E. Zhou, C. Hwang, and A. Fouad, "Derivation of stability limits using analytical sensitivity of the transient energy margin," *IEEE Trans. Power Syst.*, vol. 4, no. 4, pp. 1363–1372, 1989.

[12] M. Pai, *Power system stability: analysis by the direct method of Lyapunov*. North-Holland, 1981, vol. 3.

[13] M. Pavella and P. Murthy, "Transient stability of power systems: theory and practice," 1994.

[14] P. Kundur, *Power System Stability and Control*. McGraw-Hill, 1994.

[15] A. M. Lyapunov, "The general problem of the stability of motion," *International journal of control*, vol. 55, no. 3, pp. 531–534, 1992.

[16] A. H. El-Abiad and K. Nagappan, "Transient stability regions of multimachine power systems," *IEEE Transactions on Power Apparatus and Systems*, no. 2, pp. 169–179, 1966.

[17] N. Kakimoto, "Transient stability analysis of electric power system via lure-type lyapunov function," *Transactions of the IEEE of Japan*, vol. 98, pp. 566–604, 1978.

[18] T. Athay, R. Podmore, and S. Virmani, "A practical method fo r direc t analysi s of transien t stability," *IEE E Trans., Vol. PAS98*, pp. 573–58.

[19] D. J. Watts and S. H. Strogatz, "Collective dynamics of 'small-world'networks," *nature*, vol. 393, no. 6684, p. 440, 1998.

[20] C. Song, S. Havlin, and H. A. Makse, "Self-similarity of complex networks," *Nature*, vol. 433, no. 7024, p. 392, 2005.

[21] X. Li, "Design of transient energy automaton and study of energy flows on lattice graph," 2018.

[22] S. V. Buldyrev, R. Parshani, G. Paul, H. E. Stanley, and S. Havlin, "Catastrophic cascade of failures in interdependent networks," *Nature*, vol. 464, no. 7291, p. 1025, 2010.

[23] Y. Yang, T. Nishikawa, and A. E. Motter, "Small vulnerable sets determine large network cascades in power grids," *Science*, vol. 358, no. 6365, p. eaan3184, 2017.

[24] D. Wu, F. Ma, M. Javadi, K. Thulasiraman, E. Bompard, and J. N. Jiang, "A study

of the impacts of flow direction and electrical constraints on vulnerability assessment of power grid using electrical betweenness measures," *Physica A: Statistical Mechanics and its Applications*, vol. 466, pp. 295–309, 2017.

[25] M. E. J. Newman, "The structure and function of complex networks," *SIAM Review 45:2*, vol. 45, no. 2, pp. 167–256, 2003.

[26] R. Albert and A. Barabasi, "Statistical mechanics of complex networks," *Reviews of Modern Physics*, vol. 74, pp. 47–97, 2002.

[27] R. Zárate-Miñano, T. Van Cutsem, F. Milano, and A. J. Conejo, "Securing transient stability using time-domain simulations within an optimal power flow," *IEEE Transactions on Power Systems*, vol. 25, no. 1, pp. 243–253, 2009.

[28] P. Hines and S. Blumsack, "A centrality measure for electrical networks," in *41st annual Hawaii Int. Conf. on System Sci.*, 2008.

[29] D. Wu *et al.*, "A study of the impacts of flow direction and electrical constraints on vulnerability assessment of power grid using electrical betweenness measures," *Physica A: Statistical Mechanics and its Applications*, vol. 466, pp. 295 – 309, 2017.

[30] A. M. Kettner and M. Paolone, "On the properties of the compound nodal admittance matrix of polyphase power systems," *IEEE Transactions on Power Systems*, 2018.

[31] R. Mcnaughton, "The theory of automata: A survey," *Advances in Computers*, vol. 2, pp. 379–421, 1961.

[32] R. W. Coffin, H. E. Goheen, and W. R. Stahl, "Simulation of a turing machine on a digital computer," in *Fall Joint Computer Conference*, 1963, pp. 35–43.

[33] S. Wolfram, "Computation theory of cellular automata," *Communications in Mathematical Physics*, vol. 96, no. 1, pp. 15–57, 1984.

[34] J. Kari, "Theory of cellular automata:a survey," *Theoretical Computer Science*, vol. 334, pp. 3–33, 2005.

[35] X. S. Yang and Y. Z. L. Yang, "Cellular automata networks," in *Unconventional Computing*. Luniver Press, 2007, pp. 280–302.

[36] J. Hopcroft and J. Ullman, *Introduction to Automata Theory, Languages and Computation.* Reading, Massachusetts: Addison-Wesley, 1979.

[37] X. Li, "Design of tranient energy automaton and study of energy flows on lattice graph," Ph.D. dissertation, University of Oklahoma, 2018.

[38] A. van der Schaft, "Port-hamiltonian systems: an introductory survey," in *Proceedings of the international congress of mathematicians*, vol. 3. Citeseer, 2006, pp. 1339–1365.

[39] B. M. Maschke and A. J. van der Schaft, "Port-controlled hamiltonian systems: modelling origins and systemtheoretic properties," *IFAC Proceedings Volumes*, vol. 25, no. 13, pp. 359–365, 1992.

[40] B. Maschke and A. Van Der Schaft, "System-theoretic properties of port-controlled hamiltonian systems," *MATHEMATICAL RESEARCH*, vol. 79, pp. 349–349, 1994.

[41] B. Maschke, A. J. Van Der Schaft, and P. C. Breedveld, "An intrinsic hamiltonian formulation of network dynamics: Non-standard poisson structures and gyrators," *Journal of the Franklin institute*, vol. 329, no. 5, pp. 923–966, 1992.

[42] T. Runolfsson, "On the dynamics of three phase electrical energy systems," in *American Control Conference (ACC), 2016.* IEEE, 2016, pp. 6827–6832.

[43] S. Fiaz, D. Zonetti, R. Ortega, J. M. Scherpen, and A. Van der Schaft, "A port-hamiltonian approach to power network modeling and analysis," *European Journal of Control*, vol. 19, no. 6, pp. 477–485, 2013.

[44] A. van der Schaft, *Port-Hamiltonian Differential-Algebraic Systems.* Berlin, Heidelberg: Springer, 2013, pp. 173–226.

[45] D. Sharma *et al.*, "Electric circuit foundation of structural analysis for power systems from a network perspective," *Proc. Mediterranean Conf. on Power Gen., Trans., Distribution and Energy Conv., Croatia (accepted)*, 2018.

[46] A. van der Schaft and D. Jeltsema, "Port-hamiltonian systems theory: An introductory overview," *Foundations and Trends in Systems and Control*, vol. 1, no. 2-3, p. 173–378, Jun 2014.

[47] D. Sharma, "Electric circuit foundation for structural analysis and applications in large-scale power networks," 2019.

[48] W. Ellens, F. Spieksma, P. Van Mieghem, A. Jamakovic, and R. Kooij, "Effective graph resistance," *Linear algebra and its applications*, vol. 435, no. 10, pp. 2491–2506, 2011.

[49] D. Sharma, C. Lin, X. Luo, D. Wu, K. Thulasiraman, and J. N. Jiang, "Advanced techniques of power system restoration and practical applications in transmission grids," *Electric Power Systems Research*, vol. 182, p. 106238, 2020.

[50] Y. Xu, A. Gurfinkel, and P. Rikvold, "Architecture of the florida power grid as a complex network," *Physica A: Statistical Mechanics and its Applications*, vol. 401, pp. 130 – 140, 2014.

[51] A. Malyscheff, D. Wu, F. Ma, and J. Jiang, "A probabilistic perspective for power flow and its implication to power network analysis," in *The 50th North American Power Symposium (NAPS), Fargo*, 2018.

[52] K. Lerman and R. Ghosh, "Network structure, topology, and dynamics in generalized models of synchronization," *Physical Review E*, vol. 86, no. 2, p. 026108, 2012.

[53] D. J. Klein and M. Randić, "Resistance distance," *Journal of mathematical chemistry*, vol. 12, no. 1, pp. 81–95, 1993.

[54] D. J. Klein, "Resistance-distance sum rules," *Croatica chemica acta*, vol. 75, no. 2, pp. 633–649, 2002.

[55] K. E. Avrachenkov, J. Filar, and M. Haviv, "Singular perturbations of markov chains and decision processes," in *Handbook of Markov Decision Processes*. Springer, 2002, pp. 113–150.

[56] D. Sharma, C. Lin, X. C. Luo, D. Wu, and J. N. Jiang, "Advanced techniques of system restoration and practical applications," in *11th Int. Conf. on Power Generation, Transmission, Distribution and Energy Conversion, Dubrovnik, Croatia*, 2018.

[57] K. Hara and S. Iwasaki, "On the quantum number projection:(i). general theory,"

Nuclear Physics A, vol. 332, no. 1-2, pp. 61–68, 1979.

[58] A. R. Edmonds, *Angular momentum in quantum mechanics*. Princeton university press, 1996.

[59] E. E. Wollman, C. Lei, A. Weinstein, J. Suh, A. Kronwald, F. Marquardt, A. Clerk, and K. Schwab, "Quantum squeezing of motion in a mechanical resonator," *Science*, vol. 349, no. 6251, pp. 952–955, 2015.

[60] C. L. Fefferman, "The uncertainty principle," *Bulletin of the American Mathematical Society*, vol. 9, no. 2, pp. 129–206, 1983.

[61] H. P. Robertson, "The uncertainty principle," *Physical Review*, vol. 34, no. 1, p. 163, 1929.

[62] E. Arthurs and M. Goodman, "Quantum correlations: A generalized heisenberg uncertainty relation," *Physical review letters*, vol. 60, no. 24, p. 2447, 1988.

[63] D. Hestenes, "Spin and uncertainty in the interpretation of quantum mechanics," *American Journal of Physics*, vol. 47, no. 5, pp. 399–415, 1979.

[64] S. Blumsack, P. Hines, M. Patel, C. Barrows, and E. C. Sanchez, "Defining power network zones from measures of electrical distance," in *Power & Energy Society General Meeting, 2009. PES'09. IEEE.* IEEE, 2009, pp. 1–8.

[65] J. C. Kolecki, "Foundations of tensor analysis for students of physics and engineering with an introduction to the theory of relativity," 2005.

[66] G. Kron, "Tensor analysis of networks," *New York*, 1939.

[67] V. Vittal, A. N. Michel, and A. A. Fouad, "Power system transient stability analysis: Formulation as nearly hamiltonian systems," in *1983 American Control Conference*, June 1983, pp. 668–673.

[68] P. M. Anderson, *Power System Control and Stability*, 2nd ed. Wiley-IEEE Press, 2002.

[69] D. Wu and J. N. Jiang, "A study of total transient energy during the fault period,"

Electric Power Components and Systems, vol. 45, no. 11, pp. 1161–1172, 2017.

[70] D. Wu, F. Ma, and J. N. Jiang, "A study on relationship between power network structure and total transient energy," *Electric Power Systems Research*, vol. 143, pp. 760–770, 2017.

[71] F. Dorfler and F. Bullo, "Kron reduction of graphs with applications to electrical networks," *IEEE Transactions on Circuits and Systems I: Regular Papers*, vol. 60, no. 1, pp. 150–163, 2012.

[72] J. C. A. Barata and M. S. Hussein, "The moore–penrose pseudoinverse: A tutorial review of the theory," *Brazilian Journal of Physics*, vol. 42, no. 1-2, pp. 146–165, 2012.

[73] F. Dorfler and F. Bullo, "Synchronization of power networks: Network reduction and effective resistance," *IFAC Proceedings Volumes*, vol. 43, no. 19, pp. 197–202, 2010.